


PEDIATRIC NEUROMONITORING



Advanced Neuromonitoring Modalities on the Horizon: Detection and Management of Acute Brain Injury in Children

Tiffany S. Ko^{1*} , Eva Catennacio², Samuel S. Shin³, Joseph Stern⁴, Shavonne L. Massey², Todd J. Kilbaugh¹ and Misun Hwang⁴

© 2023 The Author(s), corrected publication 2023

Abstract

Timely detection and monitoring of acute brain injury in children is essential to mitigate causes of injury and prevent secondary insults. Increasing survival in critically ill children has emphasized the importance of neuroprotective management strategies for long-term quality of life. In emergent and critical care settings, traditional neuroimaging modalities, such as computed tomography and magnetic resonance imaging (MRI), remain frontline diagnostic techniques to detect acute brain injury. Although detection of structural and anatomical abnormalities remains crucial, advanced MRI sequences assessing functional alterations in cerebral physiology provide unique diagnostic utility. Head ultrasound has emerged as a portable neuroimaging modality for point-of-care diagnosis via assessments of anatomical and perfusion abnormalities. Application of electroencephalography and near-infrared spectroscopy provides the opportunity for real-time detection and goal-directed management of neurological abnormalities at the bedside. In this review, we describe recent technological advancements in these neurodiagnostic modalities and elaborate on their current and potential utility in the detection and management of acute brain injury.

Keywords: Pediatric ICU, Pediatric emergency medicine, Acute brain injuries, Neuroimaging, Neurophysiological monitoring, Hypoxia–ischemia, Brain, Diagnostic ultrasound

Introduction

Over the last decade, management-based improvements in survival of pediatric critical care patients have led to a shift in focus beyond survival to neuroprotection and quality of life. Primary neurologic diagnoses requiring critical care intervention occur in 26.9 per 100,000 US children per year [1]. Seizure disorders and traumatic brain injury (TBI) are the most common primary neurological diagnoses [1–3], accounting for more than 50% of all pediatric neurocritical care admissions. Neurological infection, hydrocephalus, and stroke are also common

primary neurologic admissions. TBI remains a leading cause of death and disability in children in the United States [4]. In addition to direct brain injury, cardiac or respiratory insufficiency from congenital disease or exogenous insults (e.g., infection, aspiration) may also result in secondary hypoxic–ischemic encephalopathy (HIE). Early detection of neurological vulnerability paired with targeted brain-directed management strategies is essential to mitigating the lifelong impact of pediatric brain injury.

In the event of suspected moderate or severe closed head injury in children, noncontrast head computed tomography (CT) is widely accepted as the frontline diagnostic modality to determine the presence of life-threatening intracranial injuries and skull fractures [5–8]. The development of portable CT has also extended access

*Correspondence: kotiff@chop.edu

¹ Department of Anesthesiology and Critical Care, Children's Hospital of Philadelphia, Philadelphia, USA

Full list of author information is available at the end of the article

to critically ill patients where transport is not feasible [9, 10]. However, CT imaging falls short in detection of parenchymal contusions, diffuse axonal injury, nonhemorrhagic intracranial hypertension, and perfusion abnormalities [11, 12]. In fact, frontline CT imaging may fail to detect acute ischemic stroke in as many as 47% of children [13, 14].

Due to these limitations and evidence of the elevated cancer burden in children associated with ionizing radiation exposure [15, 16], there has been increasing adoption of frontline magnetic resonance imaging (MRI) [8, 17–22] and head ultrasound (HUS) [23, 24, 25, 26, 27]. However, diagnostic MRI and HUS is only triggered following presentation of injury and is limited to snapshots over time due to equipment and staffing requirements. Delayed detection increases injury severity and, in the critical care setting, limits opportunities for optimization of management at the bedside. Continuous noninvasive neuromonitoring modalities, including electroencephalography (EEG) and near-infrared spectroscopy (NIRS), are poised to fill this critical gap to enable more timely detection, quantification, and treatment of neurological abnormalities [28–30].

In this review, we provide a technical summary of both existing and emerging MRI, HUS, EEG, and NIRS techniques and elaborate on their current and potential indications in the detection and management of acute brain injury in pediatric populations (Table 1).

Advances in Neuromonitoring

Magnetic Resonance Imaging (MRI)

In the emergent and critical care setting, rapid MRI sequences with reduced duration on the order of seconds for individual sequences and <30-min total scan time [18, 31] has made nonsedated pediatric imaging

more successful and likely underlies increased utilization in acute brain injury [17, 25, 27]. Faster acquisition techniques are increasingly being explored, in addition to the recent emergence and utilization of portable MRI scanners [32]. Brain MRI now serves as the reference standard for detection of brain injury, including stroke [14, 21, 33], status epilepticus [34], and TBI [35]. The sections below detail key advanced MRI techniques that have provided value in the diagnosis and prognostication of pediatric brain injury in the critical care setting.

Arterial Spin Labeling

Arterial spin labeling (ASL) enables noninvasive imaging of cerebral blood flow (CBF) on a voxel-by-voxel basis by detecting the arrival of magnetically tagged water molecules in blood [36, 37]. These water molecules are tagged by an inversion pulse as they transit through a cross-sectional tagging plane localized to the carotid and vertebral arteries in the neck. If the T1 relaxation time of arterial blood is either assumed or individually measured, absolute blood flow units of mL/100-g tissue/minute may be estimated using the flow-modified Bloch equation solution. A single inversion pulse tag results in ~1–2% change in signal from baseline [38]; enhancing this small signal contrast is an ongoing focus of ASL optimization.

The ability to noninvasively localize and quantify perfusion alterations provides critical physiologic information that may be used to detect acute neurological insults or monitor efficacy of therapeutic treatment. ASL has seen increasing routine adoption in adult patients with suspicion of stroke [39] and with status epilepticus [40, 41]; application in pediatric populations remains an active area of study due to the significant impact of brain maturation on optimal sequence parameters and on the accuracy of CBF quantification [42–45]. ASL can currently

Table 1 Neuromonitoring modalities for acute brain injury: limitations and emerging advancements

| | Clinical information | Anatomic | Staffed | Portable | Continuous | Other limitations | Advancements |
|------------|--|----------|---------|----------|------------|---|--|
| MRI | Whole-brain localization of soft tissue | X | X | | | Cost Patient transport | Rapid sequences Perfusion Metabolism Tractography |
| Ultrasound | Anatomical imaging of soft tissue Perfusion | X | X | X | | Field-of-view Operator variability | Low-flow sensitivity Microvascular perfusion Elastography Intracranial pressure |
| EEG | Seizure detection Sedation | | X | X | X | Electrical interference Interpretation expertise | Artifact rejection Quantitative metrics Localization |
| Optical | Cerebral oxygen saturation | | | X | X | Intersubject variability | Perfusion Oxygen metabolism Intracranial pressure Cerebral autoregulation |

provide relative information regarding perfusion across different brain regions; however, it cannot provide absolute values for CBF that could be used to classify hypoperfused, ischemic, and infarcted brain tissue.

When ASL is combined with a diffusion-weighted imaging (DWI) acquisition, a mismatch showing high diffusivity on DWI with low blood flow on ASL may help identify at-risk hypoperfused regions prior to infarct [39, 46]. ASL measurements of CBF have also demonstrated correlation with brain tumor severity grading in children [47, 48] and decreased perfusion in children with uncompensated hydrocephalus that is reversed following neurosurgical intervention [49, 50]. Evidence of the utility of ASL for seizure localization and prognostication of refractory status epilepticus in children is also emerging [51–59]. Perfusion abnormalities are observed more commonly in focal versus generalized seizures [55, 58]. Lam et al. [57] found presurgical ASL abnormalities had 100% sensitivity but 23% specificity for predicting positive histopathology results in 11 surgical patients with focal epilepsy. Further study is needed to clarify the presentation of hyperperfusion versus hypoperfusion abnormalities as a function of postictal timing, pathogenesis, and patient age.

Diffusion Tensor Imaging

Diffusion tensor imaging (DTI) is an advanced computational derivative of DWI that permits characterization of white matter structure and function [60]. Commonly reported voxel-specific DTI metrics are the fractional anisotropy (FA), reflecting the degree of directed diffusion, and the mean diffusivity (MD), the average magnitude of diffusion in all directions. With axonal injury, FA is commonly reduced and MD is elevated. Computational methods may be used to connect neighboring voxels with similar directed diffusion to reconstruct axonal fiber tracts. Advanced analysis of DTI data includes tract-based spatial statistics, tractography, and functional connectivity via application of graph theory [61].

DTI sensitivity to microstructural abnormalities and disruptions of white matter fiber tracts has shown significant correlation with functional status, even in the absence of apparent abnormalities on conventional T1 and T2 structural imaging. In neonates with HIE, severity of DTI abnormalities, present in white matter, basal ganglia, posterior limb of the internal capsule, and watershed areas, was correlated with seizure severity [62]. Significant reductions in FA observed at 3 months post injury persist up to 18 months following moderate to severe pediatric TBI, which may underlie functional deficits [63]. DTI parameters have also shown good correlation with plasma biomarkers of injury, such as

neurofilament-light and glial fibrillary acidic protein, in both clinical [64] and animal models of TBI [65]. In children with status epilepticus, DTI injury severity grade was also correlated with elevated serum S100B protein levels, a marker of brain injury [66]. Further study is necessary to determine whether DTI abnormalities may in fact precede seizure burden or result secondary to injury.

Challenges remain in improving the accuracy of tract reconstruction. DTI reconstruction based on increased directional density (250+ directions), termed high-definition fiber tractography, is capable of resolving complex fiber crossings using diffusion spectrum imaging and has demonstrated increased fidelity and robustness of tract reconstruction [67, 68]. Specifically, detailed information of white matter microstructural injury can be visualized and quantified (Fig. 1). However, further characterization is needed for pediatric brain injury given that the degree of myelination differs from adults. Because TBI pathophysiology has significant differences between pediatric and adult population, fiber tractography studies comparing the two are needed in the future.

Magnetic Resonance Spectroscopy and Imaging

Magnetic resonance spectroscopy (MRS) provides non-invasive concentration profiling of several significant metabolites, including small molecular weight amino acids, carbohydrates, fatty acids, and lipids, to aid in the detection and treatment of brain tumors, infection of the central nervous system, mild TBI, HIE, and other subclinical acute insults (Table 2) [69–73]. Although conventional MRI focuses on imaging the proton of the hydrogen molecule (^1H) in water, MRS utilizes the magnetic field signal of hydrogen protons on these other molecular species to quantify alterations in metabolism, neuronal cell death, and demyelination.

MRS yields critical diagnostic information in neonates with perinatal asphyxia in which N-acetylaspartate (NAA) concentration, the lactate (Lac)/NAA ratio, and the Lac/choline ratio have been correlated with poor outcome [74–78]. Recent results of the MARBLE trial confirm the high predictive utility of reduced thalamic NAA concentration (AUC=0.99) and elevated Lac/NAA ratio >0.22 (AUC=0.94), measured within 4–14 days after birth, for adverse neurodevelopmental outcomes at 2 years of age [79]. Significant reduction in MD and elevation of the Lac/NAA ratio are observed within the first 2 days after birth despite unremarkable findings on T1 and T2 [76]. The Lac/NAA ratio was most highly associated with outcomes at 18–22 months of age when acquired within 24–96 h of life versus 7–14 days [80].

In TBI, NAA level has been demonstrated as a measure of neuronal and axonal integrity, with reduction in the

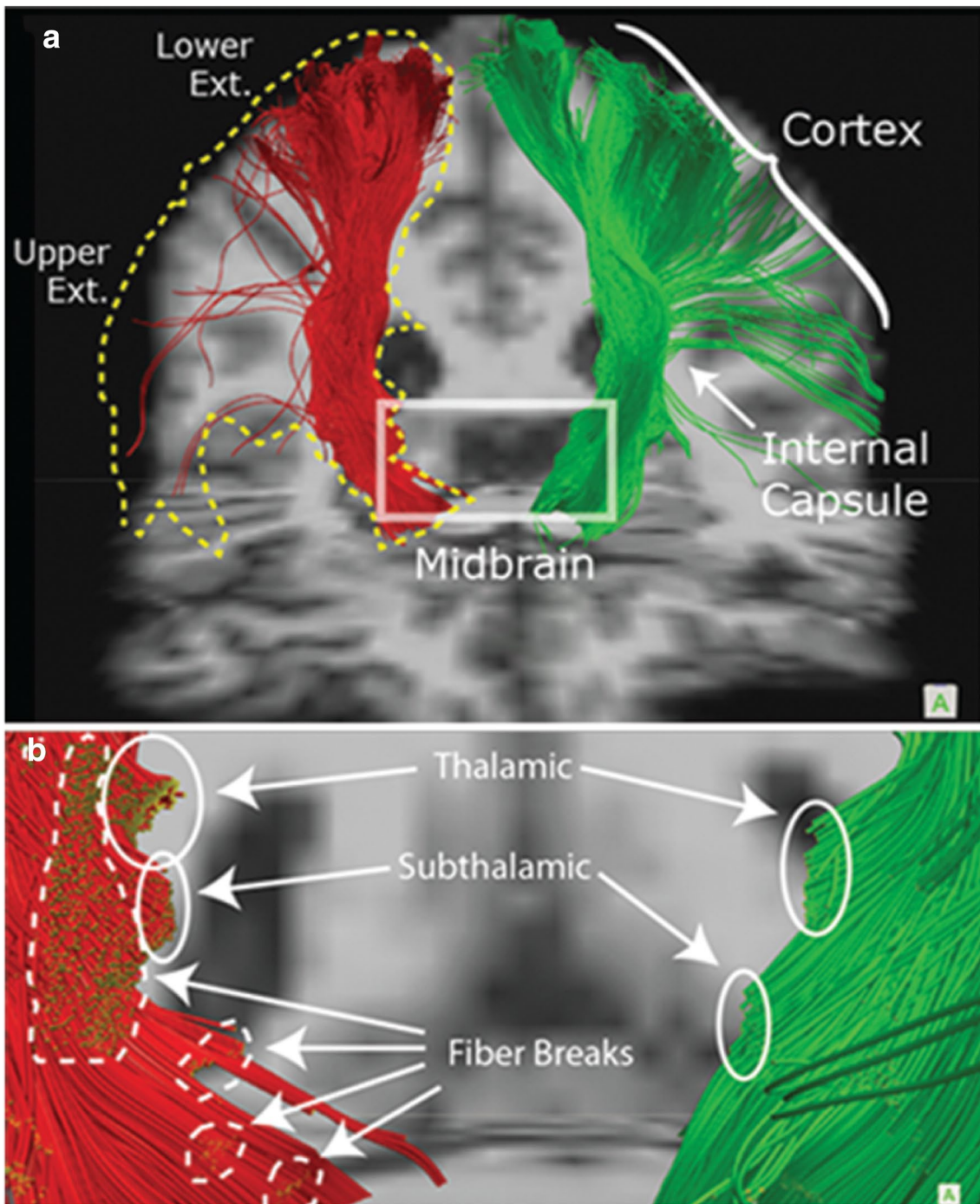


Fig. 1 Fiber tractography using diffusion imaging in a case of TBI. In this patient with severe TBI, high-definition fiber tractography showed details of white matter injury such as local disconnection in the subcortical regions (white circles) and well as gross disconnections of large regions (yellow-dotted outline). Abbreviations: TBI, traumatic brain injury. (Figure adapted from Shin et al. (2012) with permission. JNS Publishing Group holds the copyright to this figure, and subsequent use of this material requires permission from JNS Publishing Group.)

NAA level following TBI [81, 82]. An additional parameter that is widely used includes choline, which is considered a biomarker of cell membrane turnover [83]. Given

the variability of NAA levels at different time points after TBI, as well as the study participant's age, normalization, such as using the NAA/creatinine ratio or comparison

Table 2 Magnetic resonance spectroscopy: metabolites and diagnostic utility

| Metabolite | Physiology | Diagnostic utility |
|------------|---|---|
| Cho | Precursor component of cell membranes and myelin | (+) cellular proliferation; viral infection; brain tumors (-) hypothermia |
| Cr | Metabolic product of creatine phosphate breakdown during protein metabolism | (+) metabolic activity; energetic reserve; inflammation (-) pilocytic astrocytoma |
| Gln | Precursor for neuronal synthesis of glutamate | (+) acute hypoxic-ischemia; brain tumors |
| Glu | Excitatory neurotransmitter | (+) brain maturation; epileptic tissue; excitotoxicity |
| Lac | Metabolic product of anaerobic glycolysis | (+) acute hypoxic-ischemia; brain tumors |
| Lip | Fatty acid component of cell membranes | (+) apoptosis/necrosis |
| mIns | Glial metabolite | (+) gliosis; astrocytoma (-) brain maturation |
| NAA | Neuronal metabolite | (+) neuronal integrity; brain maturation (-) acute hypoxic-ischemia; apoptosis/necrosis; acute seizure |
| Suc | TCA cycle intermediate metabolite | (+) infection |

Abbreviations: Cho, Choline; Cr, Creatinine; Gln, Glutamine; Glu, Glutamate; Lac, Lactate; Lip, CH₃ (methyl) and CH₂ (methylene) group lipid molecules; mIns, myo-inositol, NAA, N-acetylaspartate; Suc, Succinate; TCA, tricarboxylic acid; (+) increase in metabolite; (-) decrease in metabolite

to an appropriately aged and post-TBI time-matched control group, is important in MRS research. MRS has also demonstrated prognostic utility in TBI with severity of NAA decline and choline and Lac increase correlated with injury severity in the acute and subacute injury period [11, 84–87]. Early detection of injury severity and characterization of associated metabolic derangements may aid in the development of neuroprotective strategies to mitigate secondary injury.

Contrast-Enhanced MRI Techniques

Contrast-enhanced MRI techniques provide high-resolution anatomical and structural information to improve diagnostic discrimination of intracranial vascular malformations, vasculitis, and brain tumors in children [88, 89]. Intravenously administered contrast agents are most commonly paramagnetic gadolinium ion complexes, which shorten relaxation times of surrounding water protons. These complexes permeate the blood–brain barrier and create positive contrast enhancements (hyperintensities) in surrounding endothelial and extravascular tissue. Within the last 5 years, several gadolinium contrast agents have received regulatory approval for use in children of all age groups [89–91]. The potential risks of gadolinium contrast administration may be offset by improved diagnostic accuracy [92–94], in particular in pediatric stroke when time-to-diagnosis is vital for the prevention of neurological injury and death, and by improved prognostication [95–97]. Alternative contrast agents, including liposomes, micelles, and inorganic nanoparticles (e.g., ferumoxytol), remain an active area of study [98, 99].

“Black-blood” T1-weighted vessel wall imaging (VW-MRI) permits contrast-enhanced visualization of periarterial vessel wall structure in the anterior circulation [100–102] and has been increasingly utilized in pediatric stroke [103]. Although a degree of linear enhancement along medium- to large-sized arteries is normal in children [104], atypical enhancement in arteries bordered by cerebrospinal fluid (CSF) and/or hemispheric asymmetry provides localized discrimination of arteriopathies [96, 105–108], which contribute to as many as 50% of pediatric arterial ischemic strokes (AIS) and are associated with higher stroke recurrence and poor outcomes [109]. In a retrospective study of 16 study participants with pediatric AIS, strong vessel wall enhancement, defined on a 3-point scale (none, mild, strong) [110], at stroke presentation was correlated with progressive arteriopathy in 83% of cases [96]. VW-MRI may also improve recognition of primary vasculitis/angiitis of the central nervous system [111, 112], which has been observed in 24% of pediatric AIS cases [113] but is likely underestimated. Continued study is needed to understand the age dependence of vessel wall enhancement and if magnitude of enhancement may be a biomarker of inflammatory disease progression.

Ultrasound

HUS is an important neuroimaging modality in the pediatric neurocritical care setting due to its portability, safety, and ability to capture real-time bedside images. In neonates and infants, the open fontanelles serve as a natural acoustic window. In children with closed fontanelles, the thin squamous portion of the temporal bone can be used as the acoustic window.

Despite the availability of advanced neuroimaging techniques, HUS, due to its unique advantages, remains a pillar of brain imaging in pediatric neurocritical care.

Technical Considerations

Ultrasound frequency waves in the MHz range are generated and transmitted into tissue by a piezoelectric transducer; the echoes reflected from the tissues are also detected by the transducer. The echoes contain spatial and contrast information, which generates electrical signals and can be quantified and extrapolated into images of internal tissues and organs. Conventional HUS techniques used include grayscale, B-mode HUS, and transcranial Doppler (TCD).

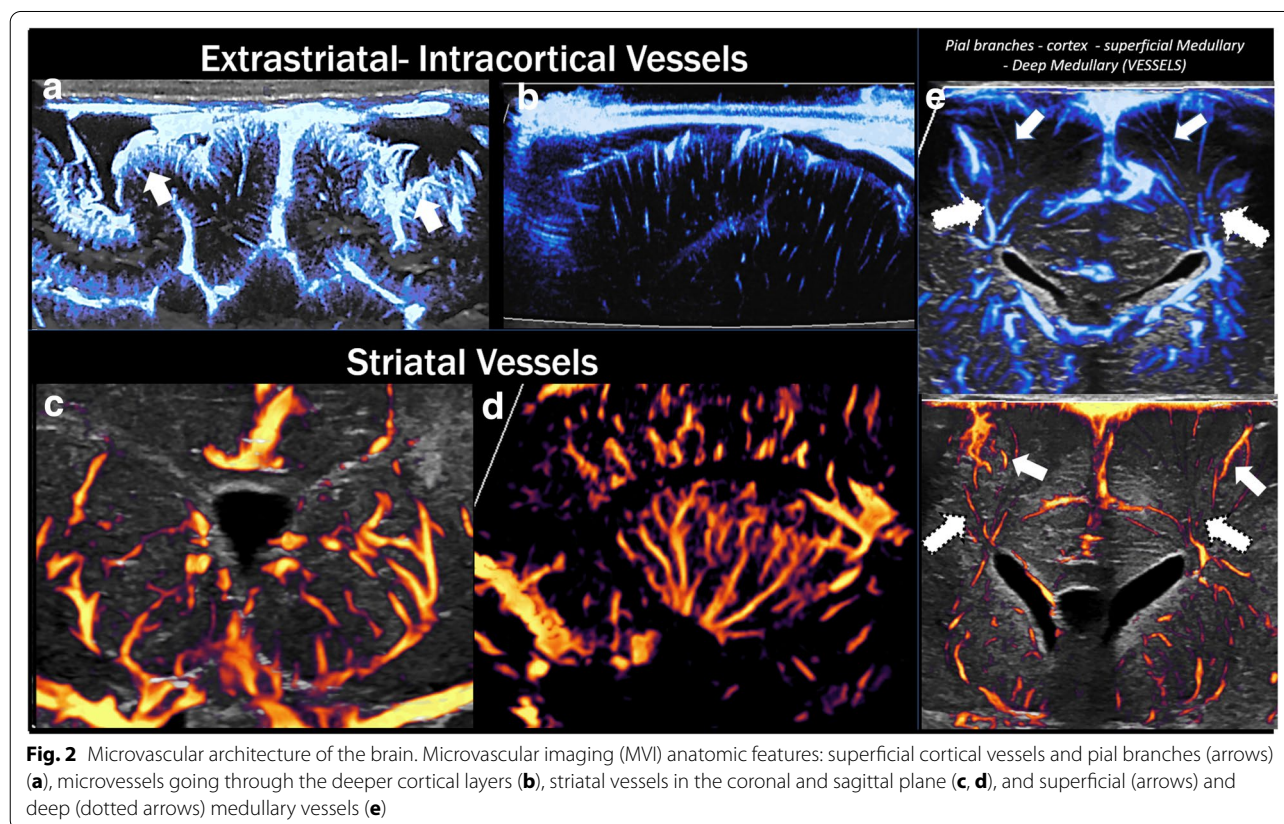
Selective filtering of returning echoes allows the visualization of information beyond that of conventional grayscale ultrasound. In this regard, Doppler ultrasound assesses frequency changes of returning echoes and can determine whether there is movement of tissue toward or away from the transducer. The technique allows assessment of blood flow through macrovessels and inferences about tissue health [114, 115]. Spectral Doppler offers quantitative flow characteristics, such as velocity, resistive index, and pulsatility. To date, TCD ultrasound has served an important role in

screening for patients with at-risk ischemia, ischemia, and/or vasospasm. Namely, TCD serves as the standard of care screening tool for patients with sickle cell [116, 117]. Major limitations of Doppler ultrasound technology include high sensitivity to motion and insensitivity to slow flow, such as that of microvessels. Emerging advanced ultrasound techniques are being studied to overcome the inherent limitations of conventional techniques.

Emerging Techniques

Microvascular Imaging Microvascular imaging (MVI) is an advanced Doppler technique that permits visualization of slow flow in cerebral microvessels (Fig. 2). In MVI, an advanced adaptive wall filter is used to suppress tissue clutter or static noise while detecting low velocity flow (<2.5 cm/s) [118, 119, 120, 121]. Two modes of MVI are available: monochrome MVI and color MVI. Monochrome MVI highlights flow in microvessels in the dark background with the grayscale ultrasound subtracted. Color MVI allows visualization of microvessels overlaid on the grayscale anatomical background.

There is emerging evidence that MVI may be used to detect cerebral microvessels in the brain, thereby attaining information on normal neurodevelopment and



functional alterations related to a variety of brain pathologies [122]. Initial studies have reported on feasibility of visualizing striatal and nonstriatal (superficial and deep cortical) microvessels using this technique [119, 120]. Age-dependent differences in the morphology of cerebral microvessels can be observed with lesser visualization and maturity of both the striatal and nonstriatal vessels in the brains of preterm versus term infants [119]. In hemispheric stroke, acute hypoperfusion or reperfusion response to initial ischemic insult can be detected, especially when the abnormality is asymmetric and/or focal in distribution [122, 123]. Real-time bedside detection could allow timely individualized management. Although MVI has predominantly been applied in infants, application in children with closed fontanelles is plausible using the temporal bone as the acoustic window.

Contrast-Enhanced Ultrasound Contrast-enhanced ultrasound (CEUS) is a technique that uses the intravenous injection of an ultrasound contrast agent called microbubbles for assessment of tissue perfusion (Fig. 3). These contrast agents can be given in bolus injections or continuous infusion, though the former is the more widely

utilized method in the clinical setting. Microbubbles oscillate on insonation and emit echoes that are detected by the transducer to create signal. Microbubbles are approximately 2–3 μm in size, about half the size of red blood cells, thereby coursing through the capillaries of organs. Commercially utilized microbubbles contain biologically inert gas in the core and phospholipid monolayer in the shell. If injected into the body, the gas is cleared through the lungs. CEUS allows spatiotemporal assessment of tissue perfusion in real time, complementing conventional ultrasound, without the need for transportation, sedation, or radiation. Dynamic perfusion kinetics are quantified using the standardized time-intensity curve, wherein signal intensity in a region of interest is quantified over time [124]. CEUS uses a low mechanical index, typically less than 0.2, to avoid microbubble destruction. Use of a curved transducer between 2 and 8 MHz allows for optimal visualization, as this frequency coincides with the resonant frequency of the microbubbles.

Although the use of CEUS in the brain is relatively new, there is great potential for quantitative and qualitative evaluation of many neurological pathologies and evaluation of cerebral perfusion for diagnostic and

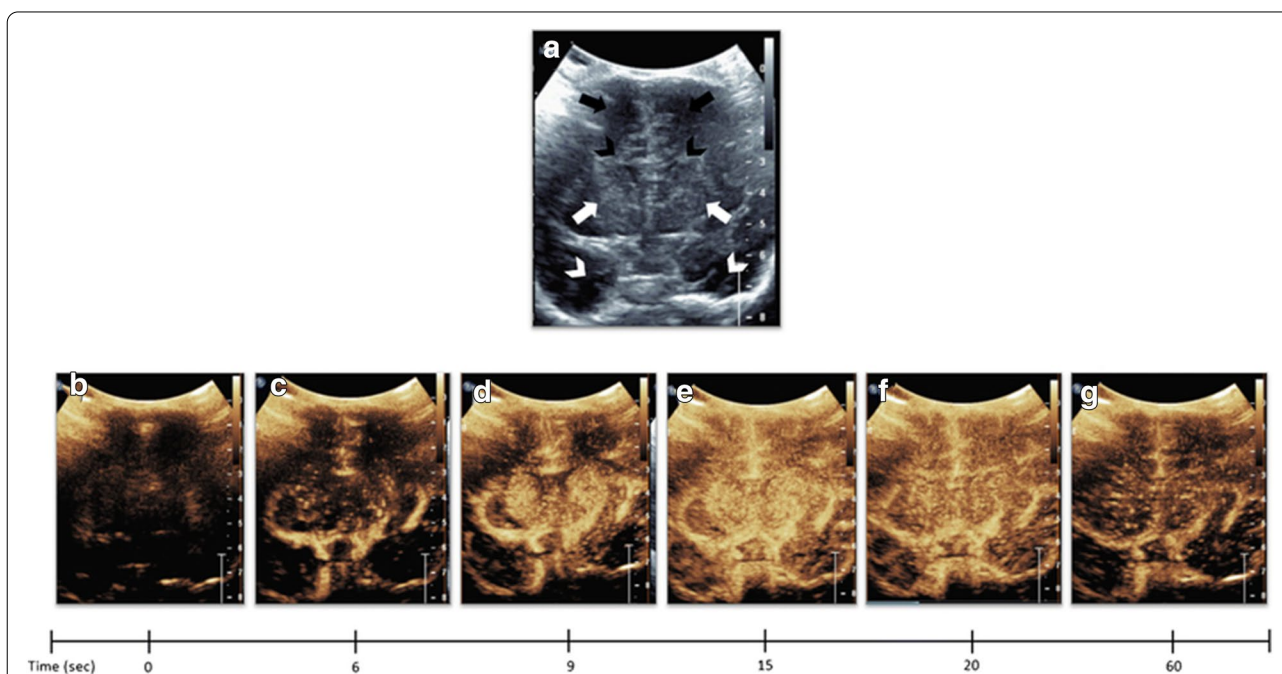


Fig. 3 Dynamic microbubble wash-in on midcoronal brain scan in a normal study participant. **a** Denotes a midcoronal grayscale ultrasound scan through the brain of a normal study participant showing bilateral frontal lobes (orange arrows), frontal horns (yellow arrowheads), basal ganglia (red arrows), and temporal lobes (white arrows). **b–g**, Demonstrates dynamic microbubble wash-in through the midcoronal slice through the brain on a contrast specific mode from the time of injection (time 0) to 1 min. Note that the microbubbles flow into the partially visualized Circle of Willis by 13 s. By 15 s, relatively more avid enhancement to the basal ganglia with respect to the remainder of the brain is seen. Further enhancement of the cortex but with relative hyperenhancement of the basal ganglia is noted at 20 s. Wash-out of contrast from both the basal ganglia and cortex begins at 25 s and further wash-out noted at 60 s. Note that Fig. 2 images were obtained with EPIQ scanner (Phillips Healthcare, Bothell, WA) and C5-1 transducer with settings of 12 Hz and MI of 0.06. (Fig. reproduced from Hwang (2019) [270] with permission.)

prognostic use. Given the inherent challenges of detecting symmetric and/or diffuse pattern injury as can be seen in hypoxic–ischemic injury, Hwang et al. assessed the feasibility of quantitative detection by evaluating the ratio of basal ganglia to cortex perfusion [125]. In stroke, hyperacute hypoperfusion or reperfusion response can be assessed. In fact, much of the CEUS studies in stroke have been in children and adults with closed fontanelles [124, 126]. In using the temporal bone as the acoustic window, it is important to recognize that the acoustic-bone impedance can lead to decreased signal on the contralateral side [127]. If using the bolus injection technique, two bolus injections and interrogation of hemispheric temporal bone each are therefore desirable so as not to attribute apparent signal reduction in the contralateral brain to injury.

A recent article by Zhang et al. has shown that cerebral microvascular flow as assessed using microbubbles can provide robust measures of intracranial pressure (ICP) and brain ischemia in hydrocephalus [128]. In this study, advanced particle tracking is applied in a neonatal porcine hydrocephalus model to track individual microbubble across thousands of ultrasound frames to derive cerebral microvascular morphology and velocity (Fig. 4). A strong correlation between cerebral microvascular velocity and ICP was observed, with incremental reduction in flow velocity with increasing pressure. Interestingly, the onset of brain ischemia coincided with drastic reduction in cortical flow. As such, spatial changes in cerebral microvascular flow can serve as a valuable biomarker of disease and help guide therapy in the future if further validated. Beyond hydrocephalus, the potential utility of CEUS has been described in a wide range of neurologic diseases, including brain tumors and vascular malformations [124].

Elastography Elastography is an advanced ultrasound technique that allows for the noninvasive assessment of brain tissue stiffness [129, 130, 131]. Brain tissue stiffness can change with many factors, including myelination, edema, and ICP. There are two primary ultrasound elastography methods used: strain-based and shear-wave-based elastography. It should be noted that strain elastography provides semiquantitative measures of brain stiffness whereas shear wave elastography provides quantitative measures of brain stiffness, such that the latter is most widely used in brain applications. In strain-based elastography, external pressure is applied by the operator, and Young's modulus is calculated from tissue displacement from the applied external pressure. Stiffer lesions deform less to external pressure and therefore have higher Young's modulus values. In shear-wave-based elastography, high-intensity acoustic waves induce perpendicu-

larly propagating shear waves from tissue, which are then captured by the ultrasound probe to measure shear wave velocity (SWV). Young's modulus is estimated from SWV; greater SWV signifies greater tissue stiffness and a greater Young's modulus value.

Brain elastography has been applied predominantly in infants due to open acoustic fontanelles. Age- and region-dependent differences in brain elasticity have been shown [132–136]. Applications in disease diagnostics remain sparse but are emerging; it has been shown that brain stiffness increases in a focal epileptic zone [137], can either increase or decrease depending on the timing of hypoxic–ischemic injury, and increases with raised ICP [138]. In situations when high ICP is suspected, elastography may serve as a useful adjunct tool (Fig. 5).

Electroencephalography (EEG)

EEG, initially developed in the 1920s [139], has traditionally been used for the diagnosis and management of epilepsy, one of the most common chronic neurologic illnesses in children [140]. However, due to exquisite temporal resolution and advances in real-time interpretation, continuous EEG (cEEG) is increasingly being utilized as a neuromonitoring tool in intensive care units for a variety of indications in both neonatal [141, 142] and pediatric/adult populations [143, 144]. The goals of monitoring are to (1) identify background patterns and features that may indicate underlying cerebral dysfunction, direct toward specific etiologies, or provide prognostic data and (2) detect and quantify electrographic seizures and assess response to treatment. It is well established that there is a large burden of EEG-only (subclinical) seizures in critically ill populations that require cEEG monitoring for detection. Review of EEG activity can identify patterns suggestive of seizures, structural abnormalities (e.g., slowing of cerebral activity in a focal region), diffuse cerebral dysfunction, or specific disease processes (e.g., extreme delta brush patterns seen in autoimmune encephalitis).

Technical Considerations

During an EEG recording, an array of electrodes is placed on the scalp (using a conductive paste and/or glue) in standardized locations (10–20 system of electrode placement); the number of electrodes used may vary by patient age and head circumference, with a sparser array used in neonates [145]. The electrical activity detected by an EEG electrode represents the summation of excitatory or inhibitory postsynaptic potentials in groups of underlying cortical pyramidal neurons firing simultaneously [146]. This generates an electrical field that diminishes in strength with increasing distance from the source of the electrical potential. Differential amplification of electrical

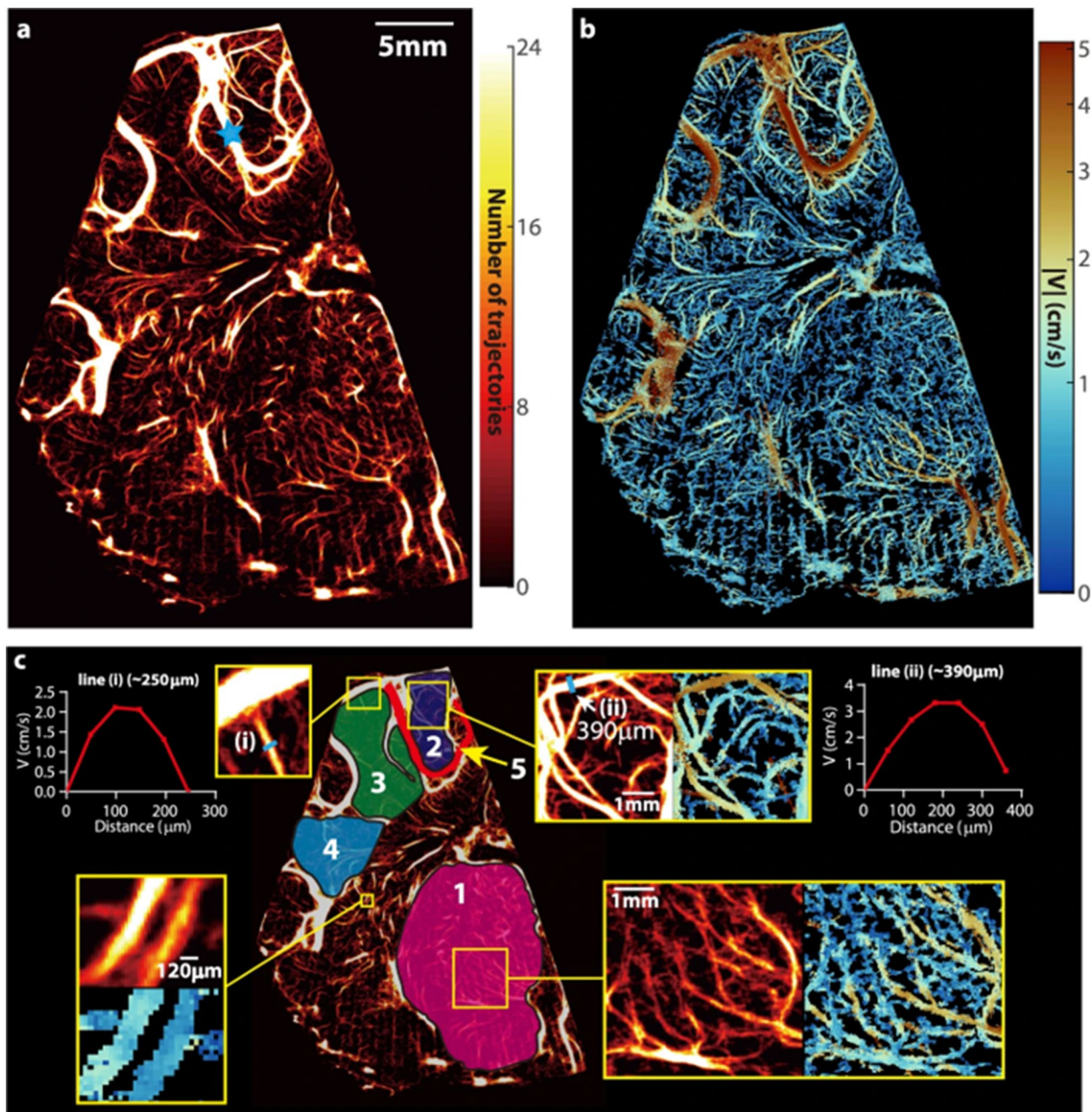


Fig. 4 Cerebral vascular map and velocity distribution for a piglet at baseline intracranial pressure. **a**, A heatmap of all the trajectories containing at least four exposures visualizing the micro- and macro-vascular distributions in a coronal plane. The blue star marks the location of pulsed-wave Doppler ultrasound measurement. **b**, The corresponding time-averaged velocity distribution. **c**, Several sub-regions are labeled for statistical analysis of perfusion, including the micro-vessels in the thalamus (#1), several parts of the cortex (#2, #3, and #4), as well as a macro blood vessel (#5). A few regions are magnified to provide a closer view of the current regions of interest. Sample velocity profiles across two different blood vessels are also provided in (c). One measurement is made for this sample case, where 5760 images are used to generate results. (Figure reproduced from Zhang et al. [128] under Creative Commons license—<http://creativecommons.org/licenses/by/4.0/>.)

potentials between pairs of inputs (either two electrodes or an electrode and a reference signal) are compared. Combinations of electrodes, called montages, aid in localizing where electrical field potentials are maximal.

Electrical waveforms themselves can be characterized by their frequency, voltage, morphology, and rhythmicity and interpreted as normal or abnormal in the context of

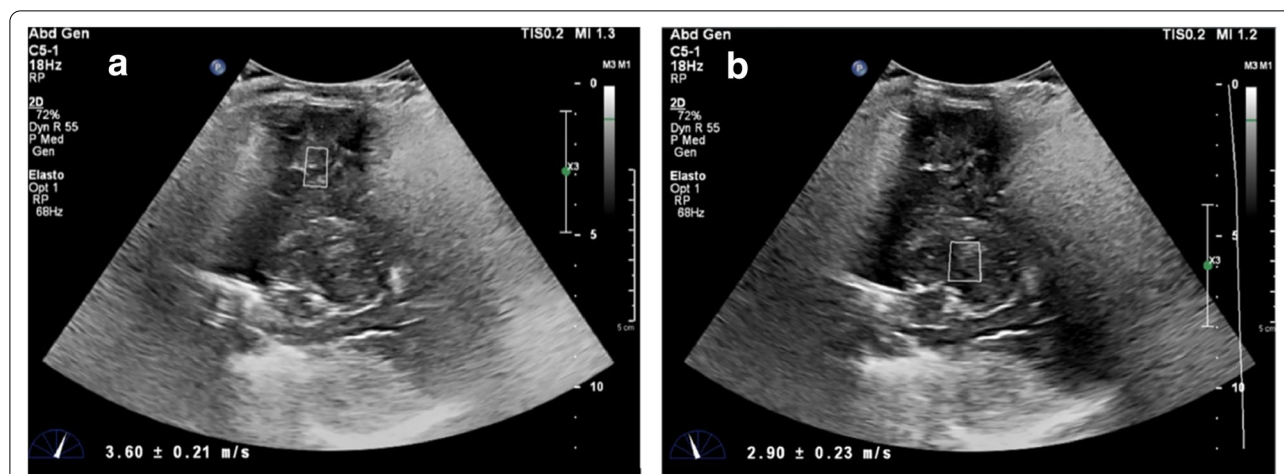


Fig. 5 Ultrasound elastography of an infant with severe anoxia. This is a 6-month-old, former 37-week gestational infant with unwitnessed cardiac arrest at home. Capillary gas pH 6.8, pCO₂ 43, pO₂ 144, and bicarbonate 3.5. End tidal CO₂ during resuscitation were in the 20 s and high 40 s. He was imaged 30 min after return of spontaneous circulation. Values were elevated in the gray and white matter 3.6 ± 0.21 m/s (**a**) and basal ganglia 2.9 ± 0.23 m/s (**b**). (Reproduced from deCampo and Hwang [130] with permission.)

age, behavioral state (awake, asleep, indeterminate), and other factors, such as medication administration.

Advanced EEG Techniques: Quantitative EEG Analysis

There is increasing interest in the application of mathematical transformations to raw EEG, termed quantitative EEG (QEEG), to enhance the efficiency of EEG interpretation, to allow for real-time bedside interpretation, and to identify subtle changes in brain activity that may not be evident on conventional intermittent review of raw waveforms by an electroencephalographer. The basis of QEEG analysis is transformation of raw time-domain (TD) EEG waveforms into a frequency-domain (FD) distribution using the fast Fourier transform (FFT); the FFT may be used to assess the relative contributions of various frequency bands of electrical brain activity to overall power (spectrograms) [147]. Amplitude integrated EEG (aEEG), in which the EEG signal from each hemisphere is filtered, rectified, and displayed as peak-to-peak amplitude on a compressed time scale, is routinely used at the bedside of high-risk critically ill neonates. aEEG has demonstrated correlations with encephalopathy severity and can be used to screen for seizures [148]. Additional analyses include assessment of rhythmicity, the degree of asymmetry between different regions, and the suppression ratio (defined as the percentage of EEG activity that falls below a set amplitude threshold).

Seizures typically manifest on FFT spectrograms as abrupt increases in power (“flames”) and rhythmicity [149]; QEEG has been used to augment cEEG review for seizure detection [150, 151]. QEEG has also demonstrated utility for the detection of ischemia related to

vasospasm following subarachnoid hemorrhage [152, 153] or during carotid endarterectomy [154] in adults. Ischemia may manifest as decreased power in faster frequencies and increased power in slower frequencies, sometimes called the alpha/delta ratio [155]. Preliminary reports in both adult and pediatric populations suggest that changes in QEEG trends may precede other clinical signs in devastating but potentially reversible conditions, such as strokes or cerebral herniation events [156–158]. Despite the longstanding availability of QEEG, patterns of use are highly variable across centers and require further standardization [159].

Optical Neuromonitoring

Optical neuromonitoring using near-infrared (NIR) light provides the unique ability for continuous noninvasive quantification of cerebral hemodynamic and metabolic risk factors for acute brain injury at the bedside [160, 161]. NIRS measurement of cerebral tissue oxygen saturation (StO₂), physiologically analogous to regional tissue oxygen saturation and the tissue oxygenation index, is the most widespread optical technique [174]. StO₂ assesses the balance of arterial oxygen delivery and tissue consumption and has repeatedly shown potential utility for rapid detection of cerebral hypoxia and ischemia. Compared to other modalities highlighted in this review, clinical NIRS devices are typically more portable and rapidly applied and do not require a clinical specialist. Ease of use has promoted increasing application in emergent and critical care settings [28, 162–180]. However, consensus on utility and standardized guidance for interpretation

remains lacking [175, 178, 181–184]. Here we provide a technical overview of cerebral NIRS to elucidate current limitations and highlight emerging techniques and diagnostics with potential impact on the management of acute brain injury.

Technical Considerations

Within tissue, NIR photons are either scattered or absorbed; scattering events are roughly 100 times more likely than absorption events. This relative “transparency” of tissue permits photons, emitted from a light source on the surface of the skin, to travel to, and back from, the brain [161, 185]. The predominance of scattering allows accurate modeling of light transport as diffusing particles, each performing a “random walk,” through tissue from a light source to a light detector in a “banana-shaped” distribution pattern (Fig. 6). The detected light encodes physiologic information from this diffuse region of tissue as a function of the tissue’s absorption and scattering. Accurate quantification of absorption is required to spectroscopically resolve relative concentrations of oxyhemoglobin and deoxyhemoglobin and compute StO_2 . Current clinical pediatric NIRS devices use continuous-wave (CW) NIR light-emitting diode light sources,

which enable compact, disposable patient interfaces but only permit signal contrast in detected light amplitude; population-based scattering assumptions are required to estimate absorption [186]. Advanced NIRS, also known as diffuse optical spectroscopy (DOS), provides improved quantitative StO_2 accuracy using increased spectral and temporal information.

Advanced NIRS/DOS Techniques In broadband or hyperspectral DOS, a CW white light source paired with a spectrometer light detector measures amplitude changes at hundreds of NIR wavelengths [187–189]. This increased spectral information provides the ability to estimate the contributions of tissue scattering, in addition to tissue chromophore absorption, to amplitude changes [190]. After accounting for tissue scattering, the high-resolution spectral absorption information permits concentration determination of multiple tissue chromophores. In addition to oxyhemoglobin and deoxyhemoglobin, more weakly absorbing tissue chromophores with potential physiologic significance, including cytochrome c oxidase (CCO), water, and lipid, may also be quantified. FD and TD DOS techniques provide the ability to quantify absolute values of tissue scattering and

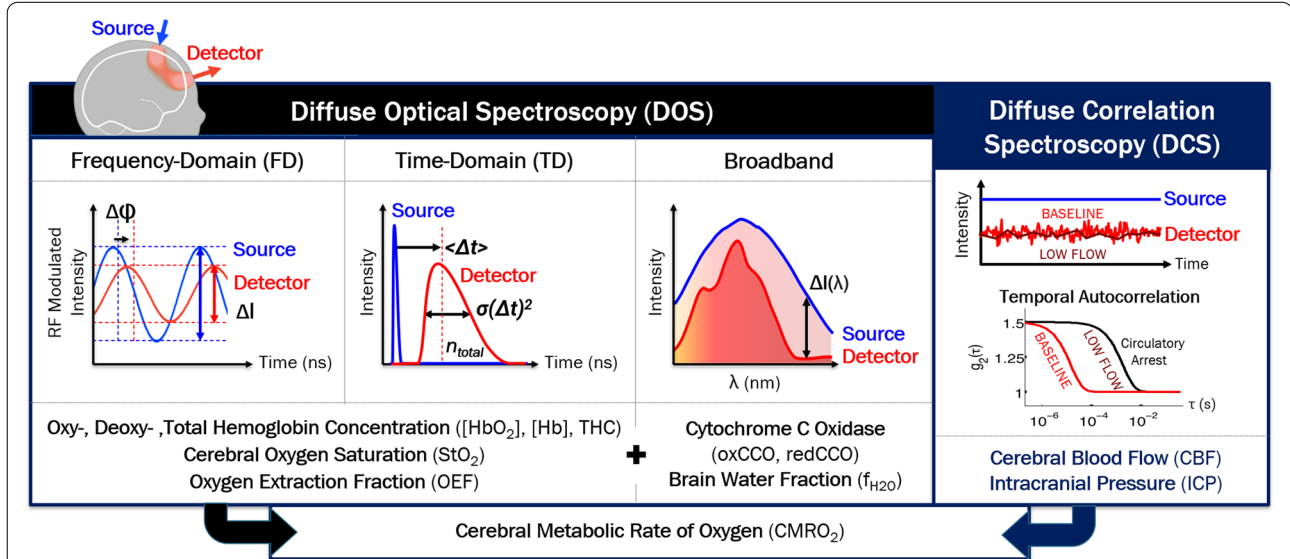


Fig. 6 Advanced optical neuromonitoring techniques and quantified physiologic parameters. Near-infrared light travels noninvasively through tissue from a light source on the surface of the skin, to the brain, and back to a light detector in a “banana”-shaped distribution. In advanced near-infrared spectroscopy (NIRS), also known as diffuse optical spectroscopy (DOS), unique properties of the detected light permit quantification of the cerebral tissue concentration of numerous physiologically significant chromophores including oxyhemoglobin and deoxyhemoglobin, water and cytochrome c oxidase (CCO) [271]. In addition to changes in intensity (used by clinical NIRS), these properties include: ϕ , phase; I , intensity; $\langle \Delta t \rangle$, mean arrival time of photons; $\sigma(\Delta t)^2$, variance of arrival times; n_{total} , total number of detected photons; and $\Delta I(\lambda)$, change in intensity across hundreds of wavelengths of NIR light. Diffuse correlation spectroscopy (DCS) is another near-infrared light technique that permits noninvasive measures of cerebral perfusion. The speed of red blood cell motion results in rapid light intensity fluctuations that may be characterized by empirically fitting for the decay of the temporal intensity autocorrelation curve (g_2); the higher the blood flow, the more rapid fluctuations occur and the more rapid the decay of the g_2 curve. This yields a blood flow index (BFI) which has been well-validated as a relative measure of cerebral blood flow. Techniques have also been developed to estimate intracranial pressure (ICP) from the pulsatile BFI waveform [251–254]

absorption properties [191–195]. In FD DOS, frequency-modulated light encodes amplitude as well as phase information. In TD DOS, an ultrafast pulse of light is attenuated and broadened as a function of absorption and scattering; time-gating of the detected pulse allows preferential selection of photons traveling deeper into tissue with greater brain sensitivity [196]. Multispectral FD and TD DOS measurements of the absorption coefficient enable absolute spectroscopic quantification of the oxyhemoglobin, deoxyhemoglobin, and total hemoglobin concentrations and more accurate calculation of StO₂ based on these absolute values compared to CW NIRS. Total hemoglobin concentration provides an additional diagnostic measure of cerebral blood volume (CBV) [197].

In contrast to broadband DOS, specialized optoelectronics are typically required for each measurement wavelength, which increases the complexity and sampling time for multispectral measurements [198]. Due to cost and footprint limitations, 2–4 measurement wavelengths are common, which precludes quantification of chromophores other than oxyhemoglobin and deoxyhemoglobin. Development of hybrid broadband and FD and TD DOS approaches is ongoing to leverage their combined advantages [199–202].

Monitoring Perfusion Diffuse correlation spectroscopy (DCS) and laser speckle contrast flowmetry are emerging optical neuromonitoring techniques that permit continuous noninvasive quantification of cerebral perfusion and remain robust in low-flow states. A cerebral blood flow index (BFI) (cm²/s) is derived from temporal and spatial characterization of rapid intensity fluctuations (termed “speckles”) resulting from the constructive and destructive interference of the scattering of coherent NIR light by moving red blood cells [160, 203–205]. In contrast to perfusion MRI and TCD, signal to noise is proportional to the amount of detected light and does not rely on intrinsic flow contrasts. Compared to DOS, quantified CBF contrasts provide improved sensitivity to the brain [206]. DCS measures of BFI have been repeatedly validated as an accurate surrogate of CBF in children and pediatric preclinical models [207, 208, 209–214] and provide sufficient temporal resolution to resolve blood flow pulsatility [215–218].

Emerging Clinical Applications

Neurometabolic Optical Monitoring Several state-of-the-art diffuse optical neuromonitoring devices have implemented combined DCS and advanced DOS techniques for investigational use in pediatric settings [191, 219–229]. The advantages of this approach are two-fold. The accuracy of DCS BFI is significantly improved by

absorption and scattering information measured by DOS [230]. Furthermore, concurrent monitoring of cerebral perfusion and oxygen saturation may be combined based on Fick’s principle to also monitor changes in the cerebral metabolic rate of oxygen in a single compact fiber optic sensor (Fig. 7) [231–233].

Longitudinal neurometabolic optical monitoring has elucidated risk factors for hypoxic–ischemic brain injury in several pediatric contexts, including during birth transition in healthy and high-risk neonates [220, 234–240], and during generalized seizures [241, 242], cardiac surgery requiring cardiopulmonary bypass [213, 225, 243, 244], and extracorporeal membrane oxygenation support [226, 245]. Quantification of oxygen delivery to the brain intra-arrest [246] (Fig. 8) and low-frequency blood flow oscillations post arrest [247] may provide novel noninvasive targets for physiologic optimization of resuscitation and postarrest care.

Broadband DOS quantification of CCO and water provides unique diagnostic utility and oxygen metabolism insights beyond the vascular compartment to intracellular mitochondria [189]. Temperature-dependent spectral features of water have been used in noninvasive brain temperature assessment [248]; water content may additionally provide diagnostic utility for monitoring of cerebral edema during extracorporeal support or following hypoxic–ischemic brain injury [249, 250].

ICP Novel optical methods have recently demonstrated promising evidence of noninvasive ICP assessment [218, 251–254]. Initial optical approaches adapted TCD ultrasound techniques [255], relating pulsatility of arterial blood pressure versus CBF for the microvasculature, measured by DCS, to quantify critical closing pressure [251, 254]. TCD cross-validation demonstrated significant correlation and concordance across a wide range of critical closing pressures (up to 65 mm Hg) in healthy adults and adults with brain injury. This technique, termed noninvasive ICP (nICP) in Flanders et al., was found to significantly correlate with invasive manometer ICP measurements in 28 infants with emergent hydrocephalus, of whom 18 (64%) fulfilled criteria for intracranial hypertension (ICP ≥ 15 mm Hg) [228]. Critically, although nICP was able to discriminate infants with intracranial hypertension, clinical diagnostic ultrasound measures (frontal-occipital horn ratio and frontotemporal horn ratio) did not (Fig. 9).

A source of uncertainty in this initial optical approach is the necessity for arterial blood pressure pulsatility measurements, which were estimated by systolic and diastolic cuff measurements. Application of advanced machine learning models may enable ICP prediction based on standalone DCS BFI or FD DOS measurements

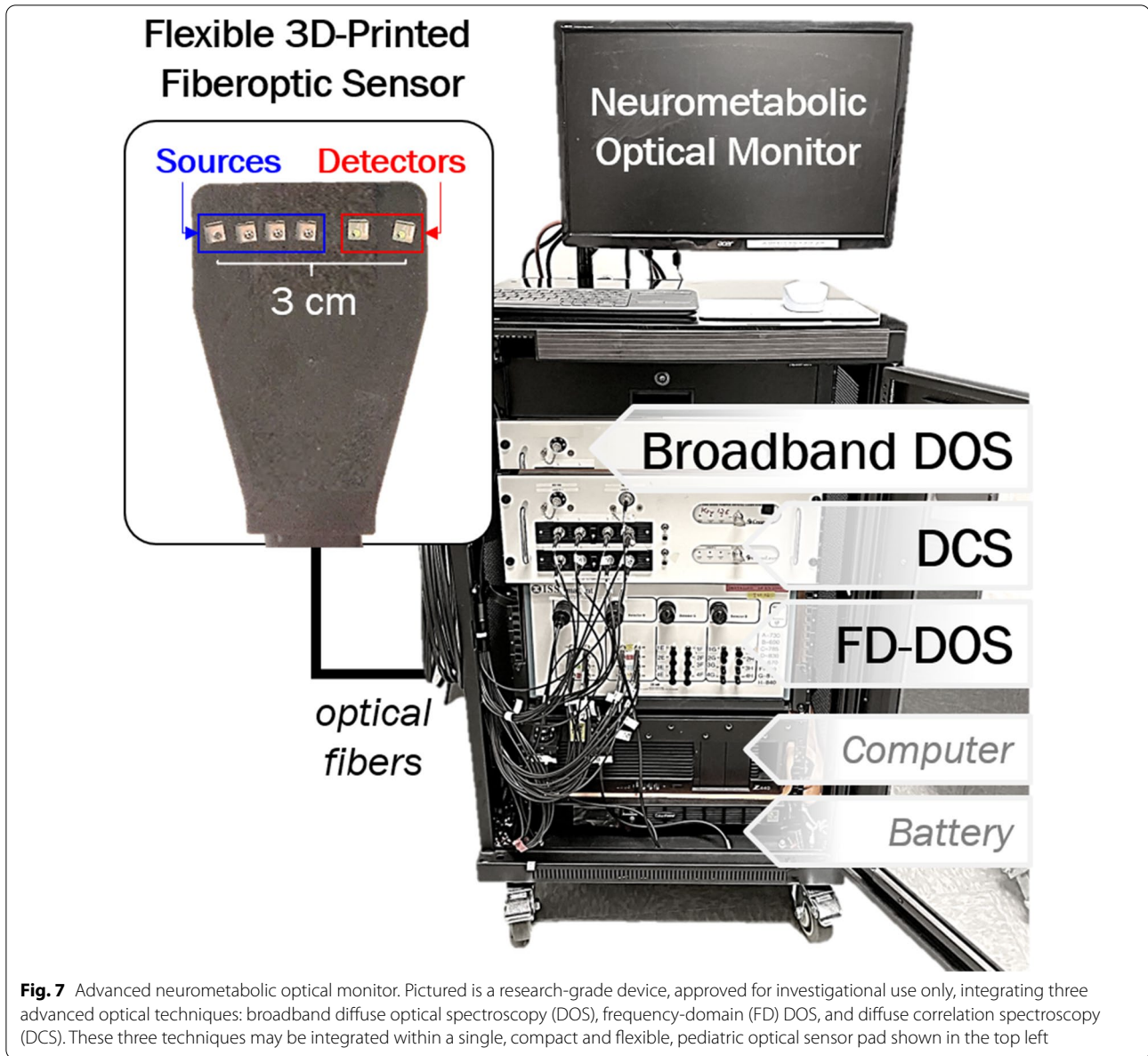
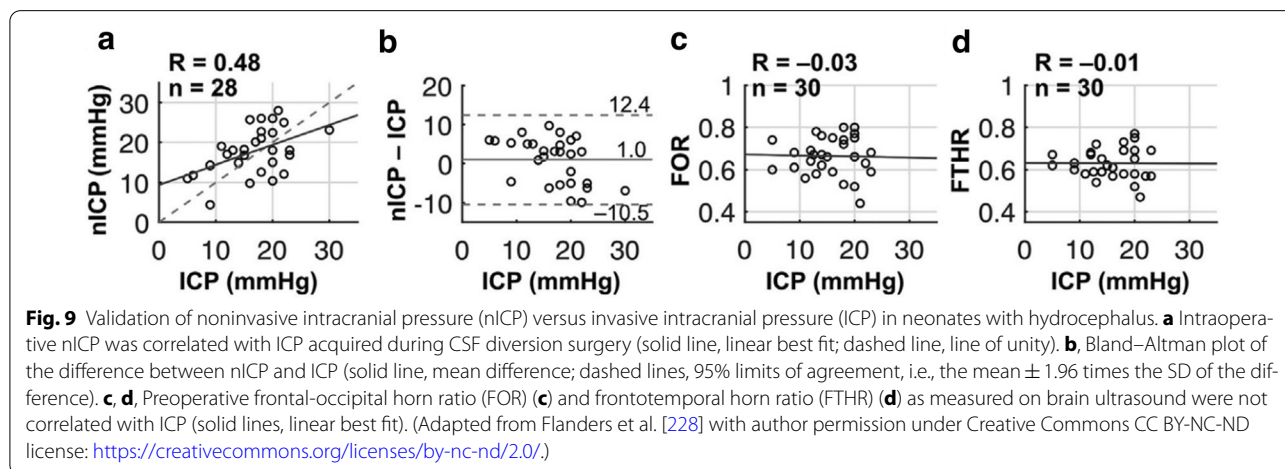
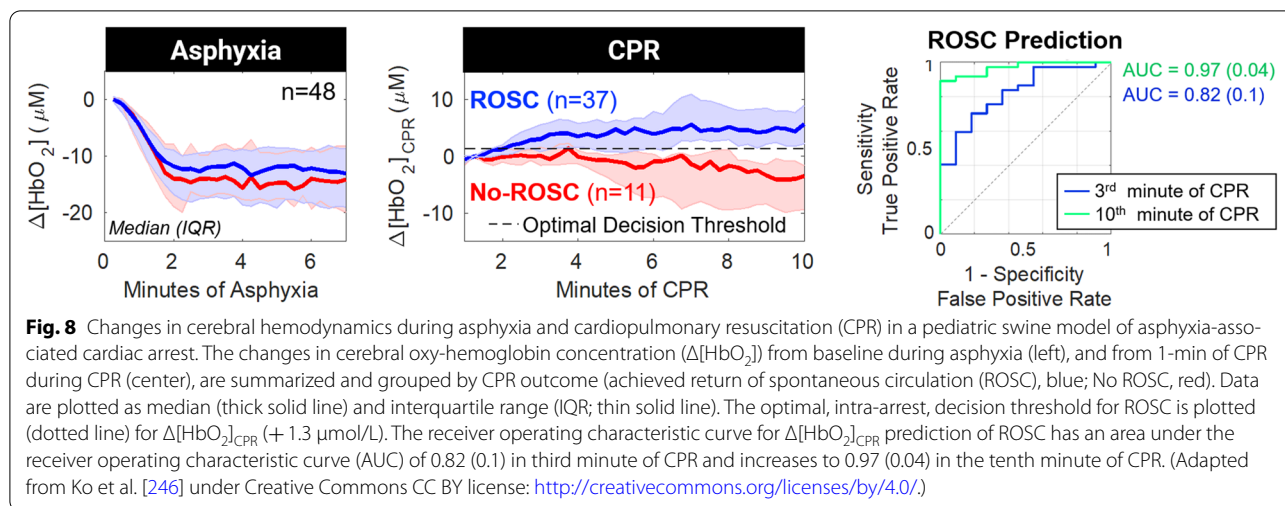


Fig. 7 Advanced neurometabolic optical monitor. Pictured is a research-grade device, approved for investigational use only, integrating three advanced optical techniques: broadband diffuse optical spectroscopy (DOS), frequency-domain (FD) DOS, and diffuse correlation spectroscopy (DCS). These three techniques may be integrated within a single, compact and flexible, pediatric optical sensor pad shown in the top left

of trends in oxyhemoglobin, deoxyhemoglobin, and total hemoglobin concentrations [252, 253, 256]. These results highlight the feasibility and potential utility for a point-of-care noninvasive optical assessment of ICP in emergent settings and as a continuous bedside monitor to improve detection and management of intracranial hypertension.

Cerebral Autoregulation Noninvasive optical assessment of cerebral autoregulation via quantification of cerebrovascular pressure reactivity has emerged as a valuable diagnostic of acute brain injury vulnerability in children [29, 173, 175, 180, 257–259]. Optical approaches to quan-

tify cerebral autoregulation in pediatric neurocritical care have commonly examined the correlation of spontaneous fluctuations in arterial blood pressure and clinical NIRS measures of CBV and StO_2 as surrogates of CBF [257, 260–262]. An excellent review of current techniques and practical recommendations for data capture, with particular emphasis on neonatal monitoring, are summarized by Rhee et al. and Vesoulis et al. [180, 257]. The application of advanced optical techniques, including the use of DCS for direct assessment of alterations in CBF [226, 263–268], may improve diagnostic utility. Assessment of pressure passivity of cerebral metabolism in term HIE infants using broadband DOS measurement of changes in oxi-



dized CCO demonstrated a significant association with MRI injury severity and neurodevelopmental outcomes at 1 year of age [239, 269].

Discussion

Advancements in noninvasive quantification of cerebral physiology provide novel insights for improved detection and management of acute brain injury in children. Emerging MRI techniques uniquely afford whole-brain spatial characterization of cerebral perfusion, metabolism, and structural abnormalities for detection and quantification of injury. This is particularly critical for localized injuries due to trauma, stroke, or neoplasms. Timing of MRI following injury and dynamic changes in MR signals with age remain a challenge for interpretation and generalizability. HUS imaging has become another essential neurodiagnostic modality due to its accessibility, safety, and portability. The emergence of advanced ultrasound techniques, such as MVI, CEUS,

and elastography, expand the quantitative and functional evaluation of many neurological pathologies. Continued optimization of acquisition parameters for efficacy and safety is underway. cEEG is critical for detection of dynamic background changes and seizures in critically ill children and neonates. QEEG is an evolving technology permitting real-time optimization of care in critically ill children. Optical neurometabolic monitoring of the brain is an emerging multiparameter modality that provides unique advantages in this respect but has limited utility in the detection of focal deep-brain injury where light is unable to penetrate. Use of cerebral NIRS for continuous StO_2 neuromonitoring has been tempered by limitations in accuracy. Emerging advanced DOS and DCS techniques provide improved quantitative accuracy and novel physiologic information for injury detection. For both ultrasound and optical techniques, neurocritical care applications have largely been limited to neonates and infants;

improving depth sensitivity is critical to characterizing focal deep-brain pathologies in older pediatric populations. Ongoing standardization of these emerging techniques will improve reproducibility and aid in necessary multicenter studies to establish high-quality evidence of clinical impact on neurodevelopmental outcomes.

Author details

¹ Department of Anesthesiology and Critical Care, Children's Hospital of Philadelphia, Philadelphia, USA. ² Division of Neurology, Department of Pediatrics, Children's Hospital of Philadelphia, Philadelphia, USA. ³ Department of Neurosurgery, Hospital of the University of Pennsylvania, Philadelphia, USA. ⁴ Department of Radiology, Children's Hospital of Philadelphia, University of Pennsylvania, Philadelphia, USA.

Author Contributions

TSK, MH: conceptualization; TSK, EC, JS: original draft preparation; SSS, SLM, TJK, MH: critical revisions; TSK, MH: manuscript finalization.

Source of support

Authors received funding support from National Institutes of Health grant R01 NS119473 (MH) and from the Children's Hospital of Philadelphia Frontier Program (TSK). No other grant funding was applied to the generation of this article.

Conflict of interest

MH received a lecture honorarium from the Korean Society of Ultrasound in Medicine (KSUM). All remaining authors declare they have no conflicts of interest.

Open Access

This article is licensed under a Creative Commons Attribution 4.0 International License, which permits use, sharing, adaptation, distribution and reproduction in any medium or format, as long as you give appropriate credit to the original author(s) and the source, provide a link to the Creative Commons licence, and indicate if changes were made. The images or other third party material in this article are included in the article's Creative Commons licence, unless indicated otherwise in a credit line to the material. If material is not included in the article's Creative Commons licence and your intended use is not permitted by statutory regulation or exceeds the permitted use, you will need to obtain permission directly from the copyright holder. To view a copy of this licence, visit <http://creativecommons.org/licenses/by/4.0/>.

Publisher's Note

Springer Nature remains neutral with regard to jurisdictional claims in published maps and institutional affiliations.

Received: 2 June 2022 Accepted: 31 January 2023

Published: 22 March 2023

References

- Williams CN, Piantino J, McEvoy C, Fino N, Eriksson CO. The burden of pediatric neurocritical care in the United States. *Pediatr Neurol.* 2018;89:31–8. <https://doi.org/10.1016/j.pediatrneurol.2018.07.013>.
- Williams CN, Eriksson CO, Kirby A, Piantino JA, Hall TA, Luther M, et al. Hospital mortality and functional outcomes in pediatric neurocritical care. *Hosp Pediatr.* 2019;9:958–66.
- DeSanti RL, Balakrishnan B, Rice TB, Pineda JA, Ferrazzano PA. The utilization of critical care resources in pediatric neurocritical care patients*. *Pediatr Crit Care Med.* 2022;23:676–86.
- Centers for Disease Control and Prevention C. The report to congress on the management of traumatic brain injury in children. *Div Unintentional Inj Prev [Internet].* 2018;1–90. <http://ovidsp.ovid.com/ovidweb.cgi?T=JS&PAGE=reference&D=emed18&NEWS=N&AN=617352660>
- Kuppermann N, Holmes JF, Dayan PS, Hoyle JD, Atabaki SM, Holubkov R, et al. Identification of children at very low risk of clinically-important brain injuries after head trauma: a prospective cohort study. *Lancet.* 2009;374:1160–70. [https://doi.org/10.1016/S0140-6736\(09\)61558-0](https://doi.org/10.1016/S0140-6736(09)61558-0).
- Araki T, Yokota H, Morita A. Pediatric traumatic brain injury: characteristic features, diagnosis, and management. *Neurol Med Chir (Tokyo).* 2017;57:82–93.
- Thompson EM, Baird LC, Selden NR. Results of a North American survey of rapid-sequence MRI utilization to evaluate cerebral ventricles in children: clinical article. *J Neurosurg Pediatr.* 2014;13:636–40.
- Ryan ME, Pruthi S, Desai NK, Falcone RA, Glenn OA, Joseph MM, et al. ACR appropriateness criteria® head trauma-child. *J Am Coll Radiol.* 2020;17:5125–37. <https://doi.org/10.1016/j.jacr.2020.01.026>.
- LaRovere KL, Brett MS, Tasker RC, Strauss KJ, Burns JP. Head computed tomography scanning during pediatric neurocritical care: diagnostic yield and the utility of portable studies. *Neurocrit Care.* 2012;16:251–7.
- Agrawal S, Hulme SL, Hayward R, Brierley J. A portable CT scanner in the pediatric intensive care unit decreases transfer-associated adverse events and staff disruption. *Eur J Trauma Emerg Surg.* 2010;36:346–52.
- Smith LGF, Milliron E, Ho ML, Hu HH, Rusin J, Leonard J, et al. Advanced neuroimaging in traumatic brain injury: an overview. *Neurosurg Focus.* 2019;47:1–9.
- Mehta H, Acharya J, Mohan AL, Tobias ME, LeCompte L, Jeevan D. Minimizing radiation exposure in evaluation of pediatric head trauma: use of rapid MR imaging. *Am J Neuroradiol.* 2016;37:11–8.
- McGlennan C, Ganesan V. Delays in investigation and management of acute arterial ischemic stroke in children. *Dev Med Child Neurol.* 2008;50:537–40.
- Christy A, Murchison C, Wilson JL. Quick brain magnetic resonance imaging with diffusion-weighted imaging as a first imaging modality in pediatric stroke. *Pediatr Neurol.* 2018;78:55–60. <https://doi.org/10.1016/j.pediatrneurol.2017.09.020>.
- Tepper SJ. Computed tomography: an increasing source of radiation exposure: Commentary. *Headache.* 2008;48:657.
- Goodman TR, Mustafa A, Rowe E. Pediatric CT radiation exposure: where we were, and where we are now. *Pediatr Radiol Pediatr Radiol.* 2019;49:469–78.
- Scheinfeld MH, Moon JY, Fagan MJ, Davoudzadeh R, Wang D, Taragin BH. MRI usage in a pediatric emergency department: an analysis of usage and usage trends over 5 years. *Pediatr Radiol Pediatr Radiol.* 2017;47:327–32.
- Ramgopal S, Karim SA, Subramanian S, Furtado AD, Marin JR. Rapid brain MRI protocols reduce head computerized tomography use in the pediatric emergency department. *BMC Pediatr BMC Pediatric.* 2020;20:1–9.
- Yue EL, Meckler GD, Fleischman RJ, Selden NR, Bardo DME, Chu O'Connor AK, et al. Test characteristics of quick brain MRI for shunt evaluation in children: an alternative modality to avoid radiation. *J Neurosurg Pediatr.* 2015;15:420–6.
- Boyle TP, Nigrovic LE. Radiographic evaluation of pediatric cerebrospinal fluid shunt malfunction in the emergency setting. *Pediatr Emerg Care.* 2015;31:435–40.
- Harrar DB, Benedetti GM, Jayakar A, Carpenter JL, Mangum TK, Chung M, et al. Pediatric acute stroke protocols in the United States and Canada. *J Pediatr.* 2022;242:220–227.e7. <https://doi.org/10.1016/j.jpeds.2021.10.048>.
- Hayes LL, Palasis S, Bartel TB, Booth TN, Iyer RS, Jones JY, et al. ACR appropriateness criteria® headache-child. *J Am Coll Radiol.* 2018;15:578–90. <https://doi.org/10.1016/j.jacr.2018.03.017>.
- Rasooly IR, Mullins PM, Alpern ER, Pines JM. US emergency department use by children, 2001–2010. *Pediatr Emerg Care.* 2014;30:602–7.
- DeFlorio RM, Shah CC. Techniques that decrease or eliminate ionizing radiation for evaluation of ventricular shunts in children with hydrocephalus. *Semin Ultrasound CT MRI.* 2014;35:365–73. <https://doi.org/10.1053/j.sult.2014.05.002>.
- Ohana O, Soffer S, Zimlichman E, Klang E. Overuse of CT and MRI in paediatric emergency departments. *Br J Radiol.* 2018;91:20170434.

26. Radhakrishnan R, Brown BP, Kralik SF, Bain D, Persohn S, Territo PR, et al. Frontal occipital and frontal temporal horn ratios: comparison and validation of head ultrasound-derived indexes with MRI and ventricular volumes in infantile ventriculomegaly. *Am J Roentgenol*. 2019;213:925–31.
27. Marin JR, Rodean J, Hall M, Alpern ER, Aronson PL, Chaudhari PP, et al. Trends in use of advanced imaging in pediatric emergency departments, 2009–2018. *JAMA Pediatr*. 2020;174:2009–18.
28. Bonifacio SL, Van Meurs K. Neonatal neurocritical care: providing brain-focused care for all at risk neonates. *Semin Pediatr Neurol*. 2019;32:100774. <https://doi.org/10.1016/j.spen.2019.08.010>.
29. Riviello JJ, Erklauer J. Neurocritical care and brain monitoring. *Neurol Clin*. 2021;39:847–66. <https://doi.org/10.1016/j.ncl.2021.04.006>.
30. Horvat CM, Mtaweh H, Bell MJ. Management of the pediatric neurocritical care patient. *Semin Neurol*. 2016;36:492–501.
31. Ha JY, Baek HJ, Ryu KH. With full basic sequences : can it be a promising way forward for. *Am J Roentgenol*. 2020;215:1–8.
32. O'Reilly T, Teeuwisse WM, de Gans D, Koolstra K, Webb AG. In vivo 3D brain and extremity MRI at 50 mT using a permanent magnet Halbach array. *Magn Reson Med*. 2021;85:495–505.
33. Lee S, Mirsky DM, Beslow LA, Amlie-Lefond C, Danehy AR, Lehman L, et al. Pathways for neuroimaging of neonatal stroke. *Pediatr Neurol*. 2017;69:37–48. <https://doi.org/10.1016/j.pediatrneurol.2016.12.008>.
34. Wickstrom R, Taraschenko O, Dilena R, Payne ET, Specchio N, Nabbout R, et al. International consensus recommendations for management of new onset refractory status epilepticus including febrile infection-related epilepsy syndrome: statements and supporting evidence. *Epilepsia*. 2022;63(11):2840–64.
35. Kessler BA, Goh JL, Pajer HB, Asher AM, Northam WT, Hung SC, et al. Rapid-sequence MRI for evaluation of pediatric traumatic brain injury: a systematic review. *J Neurosurg Pediatr*. 2021;28:278–86.
36. Telischak NA, Detre JA, Zaharchuk G. Arterial spin labeling MRI: clinical applications in the brain. *J Magn Reson Imaging*. 2015;41:1165–80.
37. Bambach S, Smith M, Morris PP, Campeau NG, Ho ML. Arterial spin labeling applications in pediatric and adult neurologic disorders. *J Magn Reson Imaging*. 2022;55:698–719.
38. Golay X, Hendrikse J, Lim TCC. Perfusion imaging using arterial spin labeling. *Top Magn Reson Imaging*. 2004;15:10–27.
39. Crisi G, Filice S, Scoditti U. Arterial spin labeling MRI to measure cerebral blood flow in untreated ischemic stroke. *J Neuroimaging*. 2019;29:193–7.
40. Matsuura K, Maeda M, Okamoto K, Araki T, Miura Y, Hamada K, et al. Usefulness of arterial spin-labeling images in periictal state diagnosis of epilepsies. *J Neurol Sci*. 2015;359:424–9. <https://doi.org/10.1016/j.jns.2015.10.009>.
41. Kim TJ, Choi JW, Han M, Kim BG, Park SA, Huh K, et al. Usefulness of arterial spin labeling perfusion as an initial evaluation of status epilepticus. *Sci Rep*. 2021;11:1–11. <https://doi.org/10.1038/s41598-021-03698-7>.
42. Blauwblomme T, Naggara O, Brunelle F, Grévent D, Puget S, Di Rocco F, et al. Arterial spin labeling magnetic resonance imaging: toward noninvasive diagnosis and follow-up of pediatric brain arteriovenous malformations. *J Neurosurg Pediatr*. 2015;15:451–8.
43. Proisy M, Corouge I, Leghouy A, Nicolas A, Charon V, Mazille N, et al. NeuroImage: clinical changes in brain perfusion in successive arterial spin labeling MRI scans in neonates with hypoxic–ischemic encephalopathy. *NeuroImage Clin*. 2019;24:101939. <https://doi.org/10.1016/j.nicl.2019.101939>.
44. Khalaf A, Iv M, Fullerton H, Wintermark M. Pediatric stroke imaging. *Pediatr Neurol*. 2018. <https://doi.org/10.1016/j.pediatrneurol.2018.05.008>.
45. Golay X, Ho M-L. Multidelay ASL of the pediatric brain. *Br J Radiol*. 2022;95(1134):20220034.
46. Pienaar R, Paldino MJ, Madan N, Krishnamoorthy KS, Alsop DC, Dehaes M, et al. A quantitative method for correlating observations of decreased apparent diffusion coefficient with elevated cerebral blood perfusion in newborns presenting cerebral ischemic insults. *Neuroimage*. 2012;63:1510–8. <https://doi.org/10.1016/j.neuroimage.2012.07.062>.
47. Yeom KW, Mitchell LA, Lober RM, Barnes PD, Vogel H, Fisher PG, et al. Arterial spin-labeled perfusion of pediatric brain tumors. *Am J Neuroradiol*. 2014;35:395–401.
48. Dangouloff-Ros V, Deroulers C, Foissac F, Badoual M, Shotar E, Grévent D, et al. Arterial spin labeling to predict brain tumor grading in children: correlations between histopathologic vascular density and perfusion MR imaging. *Radiology*. 2016;281(2):553–66.
49. Yeom KW, Lober RM, Alexander A, Cheshier SH, Edwards MSB. Hydrocephalus decreases arterial spin-labeled cerebral perfusion. *Am J Neuroradiol*. 2014;35:1433–9.
50. Krishnan P, Raybaud C, Palasamudram S, Shroff M. Neuroimaging in pediatric hydrocephalus. *Indian J Pediatr*. 2019;86:952–60.
51. Blauwblomme T, Boddart N, Chémaly N, Chiron C, Pages M, Varlet P, et al. Arterial spin labeling MRI: a step forward in non-invasive delineation of focal cortical dysplasia in children. *Epilepsy Res*. 2014;108:1932–9. <https://doi.org/10.1016/j.epilepsyres.2014.09.029>.
52. Takahara K, Morioka T, Shimogawa T, Amano T, Kawakita A, Watanabe K, et al. Perfusion imaging with arterial spin labeling in acute encephalopathy with reduced subcortical diffusion following secondary generalized status epilepticus. *Epilepsy Seizure*. 2017;9:32–9.
53. Polyanskaya MV, Demushkina AA, Vasiliev IG, Gazdieva HS, Kholin AA, Zavadenko NN, et al. Role of contrast-free MR-perfusion in the diagnosis of potential epileptogenic foci in children with focal epilepsy. *Epilepsia Paroxysmal Cond*. 2018;10:6–18.
54. Mabray P, Thewamit R, Whitehead MT, Kao A, Scafidi J, Gaillard WD, et al. Increased cerebral blood flow on arterial spin labeling magnetic resonance imaging can localize to seizure focus in newborns: a report of 3 cases. *Epilepsia*. 2018;59:e63–7.
55. Lee SM, Kwon S, Lee YJ. Diagnostic usefulness of arterial spin labeling in MR negative children with new onset seizures. *Seizure*. 2019;65:151–8. <https://doi.org/10.1016/j.seizure.2019.01.024>.
56. Uetani H, Kitajima M, Sugahara T, Muto Y, Hirai K, Kuroki Y, et al. Perfusion abnormality on three-dimensional arterial spin labeling in patients with acute encephalopathy with biphasic seizures and late reduced diffusion. *J Neurol Sci*. 2020;408:116558. <https://doi.org/10.1016/j.jns.2019.116558>.
57. Lam J, Tomaszewski P, Gilbert G, Moreau JT, Guiot MC, Albrecht S, et al. The utility of arterial spin labeling in the presurgical evaluation of poorly defined focal epilepsy in children. *J Neurosurg Pediatr*. 2021;27:243–52.
58. Pasca L, Sanvito F, Ballante E, Totaro M, Paoletti M, Bergui A, et al. Arterial spin labelling qualitative assessment in paediatric patients with MRI-negative epilepsy. *Clin Radiol*. 2021;76:942.e15–942.e23. <https://doi.org/10.1016/j.crad.2021.09.01>.
59. Tortora D, Cataldi M, Severino M, Consales A, Pacetti M, Parodi C, et al. Comparison of qualitative and quantitative analyses of MR-arterial spin labeling perfusion data for the assessment of pediatric patients with focal epilepsies. *Diagnostics*. 2022;12:1–15.
60. Feldman HM, Yeatman JD, Lee ES, Barde LHF, Gaman-Bean S. Diffusion tensor imaging: a review for pediatric researchers and clinicians. *J Dev Behav Pediatr*. 2010;31:346–56.
61. Dennis EL, Babikian T, Alger J, Rashid F, Villalon-Reina JE, Jin Y, et al. Magnetic resonance spectroscopy of fiber tracts in children with traumatic brain injury: a combined MRS—Diffusion MRI study. *Hum Brain Mapp*. 2018;39:3759–68.
62. Kline-Fath BM, Horn PS, Yuan W, Merhar S, Venkatesan C, Thomas CW, et al. Conventional MRI scan and DTI imaging show more severe brain injury in neonates with hypoxic–ischemic encephalopathy and seizures. *Early Hum Dev*. 2018;122:8–14. <https://doi.org/10.1016/j.earlhdev.2018.05.008>.
63. Wilde EA, Ayoub KW, Bigler ED, Chu ZD, Hunter JV, Wu TC, et al. Diffusion tensor imaging in moderate-to-severe pediatric traumatic brain injury: changes within an 18 month post-injury interval. *Brain Imaging Behav*. 2012;6:404–16.
64. Shahim P, Politis A, van der Merwe A, Moore B, Chou YY, Pham DL, et al. Neurofilament light as a biomarker in traumatic brain injury. *Neurology*. 2020;95:e610–22.
65. Shin S, Hefti MM, Mazandi VM, Issadore DA, Meaney D, Christman Schneider ALLC, et al. Plasma neurofilament light and glial Fibrillary acidic protein levels over 30 days in a porcine model of traumatic brain injury. *J Neurotrauma*. 2022;39(13–14):935–43.
66. Gunawan PI, Saharso D, Purnama SD. Correlation of serum S100B levels with brain magnetic resonance imaging abnormalities in children with status epilepticus. *Korean J Pediatr*. 2019;62:281–5.

67. Shin SS, Ynen TV, Pathak S, Jarbo K, Hricik AJ, Maserati M, et al. High-definition fiber tracking for assessment of neurological deficit in a case of traumatic brain injury: finding, visualizing, and interpreting small sites of damage. *Case report J Neurosurg.* 2012;116:1062–9.
68. Shin S, Okonkwo D, Schneider W, Verstynen T. Using high resolution white matter mapping to detect traumatic brain injury. *Neurosurg News: Univ Pittsburgh.* 2012;13:2012.
69. Panigrahy A, Nelson MD, Blüml S. Magnetic resonance spectroscopy in pediatric neuroradiology: clinical and research applications. *Pediatr Radiol.* 2010;40:3–30.
70. Liserre R, Pinelli L, Gasparotti R. MR spectroscopy in pediatric neuroradiology. *Transl Pediatr.* 2021;11:169–200.
71. Whitehead MT, Bluml S. Proton and multinuclear spectroscopy of the pediatric brain. *Magn Reson Imaging Clin N Am.* 2021;29:543–55. <https://doi.org/10.1016/j.mric.2021.06.006>.
72. Aida N. An invited review for the special 20th anniversary issue of MRMS1H-MR spectroscopy of the early developmental brain, neonatal encephalopathies, and neurometabolic disorders. *Magn Reson Med Sci.* 2022;21:9–28.
73. Blüml S, Saunders A, Tamrazi B. Proton MR spectroscopy of pediatric brain disorders. *Diagnostics.* 2022;12(6):1462.
74. Zarifi MK, Astrakas LG, Poussaint TY, Du Plessis A, Zurakowski D, Tzika AA. Prediction of adverse outcome with cerebral lactate level and apparent diffusion coefficient in infants with perinatal asphyxia. *Radiology.* 2002;225:859–70.
75. Alderliesten T, De Vries LS, Benders MJNL, Koopman C, Groenendaal F. MR imaging and outcome of term neonates with perinatal asphyxia: Value of diffusion-weighted MR imaging and 1 H MR spectroscopy. *Radiology.* 2011;261:235–42.
76. Barkovich AJ, Miller SP, Bartha A, Newton N, Hamrick SEG, Mukherjee P, et al. MR imaging, MR spectroscopy, and diffusion tensor imaging of sequential studies in neonates with encephalopathy. *Am J Neuroradiol.* 2006;27:533–47.
77. Penrice J, Cady EB, Lorek A, Wylezinska M, Amess PN, Aldridge RF, et al. Proton magnetic resonance spectroscopy of the brain in normal preterm and term infants, and early changes after perinatal hypoxia-ischemia. *Pediatr Res.* 1996;40:6–14.
78. Alderliesten T, De Vries LS, Staats L, Van Haastert IC, Weeke L, Benders MJNL, et al. MRI and spectroscopy in (near) term neonates with perinatal asphyxia and therapeutic hypothermia. *Arch Dis Child Fetal Neonatal Ed.* 2017;102:F147–52.
79. Lally PJ, Montaldo P, Oliveira V, Soe A, Swamy R, Bassett P, et al. Magnetic resonance spectroscopy assessment of brain injury after moderate hypothermia in neonatal encephalopathy: a prospective multicentre cohort study. *Lancet Neurol.* 2019;18:35–45.
80. Shibasaki J, Niwa T, Piedvache A, Tomiyasu M, Morisaki N, Fujii Y, et al. Comparison of predictive values of magnetic resonance biomarkers based on scan timing in neonatal encephalopathy following therapeutic hypothermia. *J Pediatr.* 2021;239:101–109.e4.
81. Holshouser BA, Tong KA, Ashwal S. Proton MR spectroscopic imaging depicts diffuse axonal injury in children with traumatic brain injury. *Am J Neuroradiol.* 2005;26:1276–85.
82. Holshouser B, Pivonka-Jones J, Nichols JG, Oyoyo U, Tong K, Ghosh N, et al. Longitudinal metabolite changes after traumatic brain injury: a prospective pediatric magnetic resonance spectroscopic imaging study. *J Neurotrauma.* 2019;36:1352–60.
83. Shekdar K, Wang DJ. Role of magnetic resonance spectroscopy in evaluation of congenital/developmental brain abnormalities. *Semin Ultrasound, CT MRI.* 2011;32:510–38. <https://doi.org/10.1053/j.sult.2011.08.001>.
84. Aaen GS, Holshouser BA, Sheridan C, Colbert C, McKenney M, Kido D, et al. Magnetic resonance spectroscopy predicts outcomes for children with nonaccidental trauma. *Pediatrics.* 2010;125:295–303.
85. Brown M, Baradaran H, Christos PJ, Wright D, Gupta A, Tsiouris AJ. Magnetic resonance spectroscopy abnormalities in traumatic brain injury: a meta-analysis. *J Neuroradiol.* 2018;45:123–9. <https://doi.org/10.1016/j.neurad.2017.09.004>.
86. Holshouser BA, Proton MR. Spectroscopy after acute central nervous system injury. *Radiology.* 1997;202:487–96.
87. Babikian T, Freier MC, Ashwal S, Riggs ML, Burley T, Holshouser BA. MR spectroscopy: predicting long-term neuropsychological outcome following pediatric TBI. *J Magn Reson Imaging.* 2006;24:801–11.
88. Knauth M, Forsting M, Hartmann M, Heiland S, Balzer T, Sartor K. MR enhancement of brain lesions: Increased contrast dose compared with magnetization transfer. *Am J Neuroradiol.* 1996;17:1853–9.
89. Gale EM, Caravan P, Rao AG, McDonald RJ, Winfeld M, Fleck RJ, et al. Gadolinium-based contrast agents in pediatric magnetic resonance imaging. *Pediatr Radiol Pediatr Radiology.* 2017;47:507–21.
90. Rosenfeld EH, Sola R, Yu Y, St. Peter SD, Shah SR. Battery ingestions in children: VARIATIONS in care and development of a clinical algorithm. *J Pediatr Surg.* 2018;53:1537–41. <https://doi.org/10.1016/j.jpedsurg.2018.01.017>.
91. Noda SM, Oztek MA, Stanescu AL, Maloney E, Shaw DWW, Iyer RS. Gadolinium retention: should pediatric radiologists be concerned, and how to frame conversations with families. *Pediatr Radiol Pediatr Radiol.* 2022;52:345–53.
92. Shah CC, Spampinato MV, Parmar HA, Raslan OA, Tomà P, Lin DDM, et al. Safety and diagnostic efficacy of gadoteridol for magnetic resonance imaging of the brain and spine in children 2 years of age and younger. *Pediatr Radiol Pediatr Radiology.* 2021;51:1895–906.
93. Braun J, Busse R, Darmon-Kern E, Heine O, Auer J, Meyl T, et al. Baseline characteristics, diagnostic efficacy, and peri-examination safety of IV gadoteric acid MRI in 148,489 patients. *Acta Radiol.* 2020;61:910–20.
94. Robertson RL, Palasis S, Rivkin MJ, Pruthi S, Bartel TB, Desai NK, et al. ACR appropriateness criteria® cerebrovascular disease-child. *J Am Coll Radiol.* 2020;17:S36–54.
95. Hipp SJ, Steffen-Smith E, Hammoud D, Shih JH, Bent R, Warren KE. Predicting outcome of children with diffuse intrinsic pontine gliomas using multiparametric imaging. *Neuro Oncol.* 2011;13:904–9.
96. Stence NV, Pabst LL, Hollatz AL, Mirsky DM, Herson PS, Poisson S, et al. Predicting progression of intracranial arteriopathies in childhood stroke with vessel wall imaging. *Stroke.* 2017;48:2274–7.
97. Withey SB, MacPherson L, Oates A, Powell S, Novak J, Abernethy L, et al. Dynamic susceptibility-contrast magnetic resonance imaging with contrast agent leakage correction aids in predicting grade in pediatric brain tumours: a multicenter study. *Pediatr Radiol.* 2022;52:1134–49. <https://doi.org/10.1007/s00247-021-05266-7>.
98. Daldrup-Link HE, Theruvath AJ, Rashidi A, Iv M, Majzner RG, Spunt SL, et al. How to stop using gadolinium chelates for magnetic resonance imaging: clinical-translational experiences with ferumoxytol. *Pediatr Radiol Pediatr Radiology.* 2022;52:354–66.
99. Guido C, Baldari C, Maiorano G, Mastronuzzi A, Carai A, Quintarelli C, et al. Nanoparticles for diagnosis and target therapy in pediatric brain cancers. *Diagnostics.* 2022;12(1):173.
100. Yuan C, Lin E, Millard J, Hwang JN. Closed contour edge detection of blood vessel lumen and outer wall boundaries in black-blood MR images. *Magn Reson Imaging.* 1999;17:257–66.
101. Swartz RH, Bhuta SS, Farb RI, Agid R, Willinsky RA, Terbrugge KG, et al. Intracranial arterial wall imaging using high-resolution 3-tesla contrast-enhanced MRI. *Neurology.* 2009;72:627–34.
102. Tan HW, Chen X, Maingard J, Barras CD, Logan C, Thijs V, et al. Intracranial vessel wall imaging with magnetic resonance imaging: current techniques and applications. *World Neurosurg.* 2018;112:186–98. <https://doi.org/10.1016/j.wneu.2018.01.083>.
103. Mossa-Basha M, Zhu C, Wu L. Vessel wall MR imaging in the pediatric head and neck. *Magn Reson Imaging Clin N Am.* 2021;29:595–604.
104. Mineyko A, Kirton A, Ng D, Wei XC. Normal intracranial periarterial enhancement on pediatric brain MR imaging. *Neuroradiology.* 2013;55:1161–9.
105. Mossa-Basha M, Shibata DK, Hallam DK, De Havenon A, Hippe DS, Becker KJ, et al. Added value of vessel wall magnetic resonance imaging for differentiation of nonocclusive intracranial vasculopathies. *Stroke.* 2017;48:3026–33.
106. Dlamini N, Yau I, Muthusami P, Mikulis DJ, Elbers J, Slim M, et al. Arterial wall imaging in pediatric stroke. *Stroke.* 2018;49:891–8.
107. Song JW, Obusez EC, Raymond SB, Rafia SD, Schaefer PW, Romero JM. Vessel wall MRI added to MR angiography in the evaluation of suspected vasculopathies. *J Neuroimaging.* 2019;29:454–7.
108. Sung J, Lee D, Song JY, Lee J, Kim JH, Lee J. The value of high-resolution vessel wall magnetic resonance imaging in the diagnosis and

- management of primary angiitis of the central nervous system in children. *Ann Child Neurol*. 2021;29:159–67.
109. Rafay MF, Shapiro KA, Surmava AM, Deveber GA, Kirton A, Fullerton HJ, et al. Spectrum of cerebral arteriopathies in children with arterial ischemic stroke. *Neurology*. 2020;94:E2479–90.
 110. Obusec EC, Hui F, Hajj-ali RA, Cerejo R, Calabrese LH, Hammad T, et al. High-resolution MRI vessel wall imaging: spatial and temporal patterns of reversible cerebral vasoconstriction syndrome and central nervous system vasculitis. *Am J Neuroradiol*. 2014;35:1527–32.
 111. Twilt M, Benseler SM. Central nervous system vasculitis in adults and children. *Handb Clin Neurol*. 2016. <https://doi.org/10.1016/B978-0-444-63432-0.00016-5>.
 112. Smitka M, Bruck N, Engelland K, Hahn G, Knoefler R, von der Hagen M. Clinical perspective on primary angiitis of the central nervous system in childhood (cPACNS). *Front Pediatr*. 2020;8:1–12.
 113. Fullerton HJ, Wu YW, Sidney S, Johnston SC. Risk of recurrent childhood arterial ischemic stroke in a population-based cohort: the importance of cerebrovascular imaging. *Pediatrics*. 2007;119:495–501.
 114. Coltrera MD. Ultrasound physics in a nutshell. *Otolaryngol Clin North Am*. 2010;43:1149–59. <https://doi.org/10.1016/j.otc.2010.08.004>.
 115. Ziskin MC. Fundamental physics of ultrasound and its propagation in tissue. *Radiographics*. 1993;13:705–9.
 116. Adams R, McKie V, Nichols F, Carl E, Zhang D-L, McKie K, et al. The use of transcranial ultrasonography to predict stroke in sickle cell disease. *N Engl J Med*. 1992;326:605–10.
 117. Purkayastha S, Sorond F. Transcranial doppler ultrasound: technique and application. *Semin Neurol*. 2012;32:411–20.
 118. Artul S, Nseir W, Armaly Z, Soudack M. Superb microvascular imaging: Added value and novel applications. *J Clin Imaging Sci*. 2017;7:45.
 119. Barletta A, Balbi M, Surace A, Caroli A, Radaelli S, Musto F, et al. Cerebral superb microvascular imaging in preterm neonates: in vivo evaluation of thalamic, striatal, and extrastriatal angioarchitecture. *Neuroradiology*. 2021;63:1103–12.
 120. Goeral K, Hojreh A, Kasprian G, Klebermass-Schrehof K, Weber M, Mitter C, et al. Microvessel ultrasound of neonatal brain parenchyma: feasibility, reproducibility, and normal imaging features by superb microvascular imaging (SMI). *Eur Radiol*. 2019;29:2127–36.
 121. Park AY, Seo BK. Up-to-date Doppler techniques for breast tumor vascularity: superb microvascular imaging and contrast-enhanced ultrasound. *Ultrasonography*. 2018;37(2):98.
 122. Hwang M, Haddad S, Tierradentro-Garcia LO, Alves CA, Taylor GA, Darge K. Current understanding and future potential applications of cerebral microvascular imaging in infants. *Br J Radiol*. 2022;95:20211051.
 123. Steggerda SJ, de Vries LS. Neonatal stroke in premature neonates. *Semin Perinatol*. 2021;45:151471. <https://doi.org/10.1016/j.sempri.2021.151471>.
 124. Hwang M, Barnewolt CE, Jünger J, Prada F, Sridharan A, Didier RA. Contrast-enhanced ultrasound of the pediatric brain. *Pediatr Radiol*. 2021. <https://doi.org/10.1007/s00247-021-04974-4>.
 125. Hwang M, Sridharan A, Darge K, Riggs B, Sehgal C, Flibotte J, et al. Novel quantitative contrast-enhanced ultrasound detection of hypoxic ischemic injury in neonates and infants: pilot study 1. *J Ultrasound Med*. 2019;38:2025–38.
 126. Meairs S. Contrast-enhanced ultrasound perfusion imaging in acute stroke patients. *Eur Neurol*. 2008;59(Suppl. 1):17–26.
 127. Hwang M, Tierradentro-Garcia LO. A concise guide to transtemporal contrast-enhanced ultrasound in children. *J Ultrasound [Internet]*. 2022; <http://www.ncbi.nlm.nih.gov/pubmed/35567704>
 128. Zhang Z, Hwang M, Kilbaugh TJ, Sridharan A, Katz J. Cerebral microcirculation mapped by echo particle tracking velocimetry quantifies the intracranial pressure and detects ischemia. *Nat Commun*. 2022;13:1–15.
 129. Sigrist RMS, Liau J, El KA, Chammas MC, Willmann JK. Ultrasound elastography: review of techniques and clinical applications. *Theranostics*. 2017;7(5):1303.
 130. deCampo D, Hwang M. Characterizing the neonatal brain with ultrasound elastography. *Pediatr Neurol*. 2018;86:19–26.
 131. Freeman CW, Hwang M. Advanced ultrasound techniques for neuroimaging in pediatric critical care: a review. *Children*. 2022;9(2):170.
 132. Kim HG, Park MS, Lee JD, Park SY. Ultrasound elastography of the neonatal brain: preliminary study. *J Ultrasound Med*. 2017;36:1313–9.
 133. Albayrak E, Kasap T. Evaluation of neonatal brain parenchyma using 2-dimensional shear wave elastography. *J Ultrasound Med*. 2018;37:959–67.
 134. El-Ali AM, Subramanian S, Krofchik LM, Kephart MC, Squires JH. Feasibility and reproducibility of shear wave elastography in pediatric cranial ultrasound. *Pediatr Radiol*. 2020;50:990–6.
 135. Wang J, Zhang Z, Xu X, Lu X, Wu T, Tong M. Real-time shear wave elastography evaluation of the correlation between brain tissue stiffness and body mass index in premature neonates. *Transl Pediatr*. 2021;10:3230–6.
 136. Yang H, Li H, Liao J, Yuan X, Shi C, Liang W. Compression elastography and shear wave ultrasound elastography for measurement of brain elasticity in full-term and premature neonates: a prospective study. *J Ultrasound Med*. 2022;42(1):221–31.
 137. Chan HW, Pressler R, Uff C, Gunny R, St Piers K, Cross H, et al. A novel technique of detecting MRI-negative lesion in focal symptomatic epilepsy: intraoperative shearwave elastography. *Epilepsia*. 2014;55:30–3.
 138. Dirrichs T, Meiser N, Panek A, Trepels-Kotteck S, Orlikowsky T, Kuhl CK, et al. Transcranial shear wave elastography of neonatal and infant brains for quantitative evaluation of increased intracranial pressure. *Invest Radiol*. 2019;54:719–27.
 139. Stone JL, Hughes JR. Early history of electroencephalography and establishment of the American clinical neurophysiology society. *J Clin Neurophysiol LWW*. 2013;30:28–44.
 140. Aaberg KM, Gunnes N, Bakken IJ, Soraas CL, Berntsen A, Magnus P, et al. Incidence and prevalence of childhood epilepsy: a nationwide cohort study. *Pediatrics*. 2017;139:e20163908.
 141. Shellhaas RA, Chang T, Tsuchida T, Scher MS, Riviello JJ, Abend NS, et al. The American clinical neurophysiology society's guideline on continuous electroencephalography monitoring in neonates. *J Clin Neurophysiol*. 2011;28:611–7. <https://doi.org/10.1097/WNP.0b013e31823e96d7>.
 142. Tsuchida TN, Wusthoff CJ, Shellhaas RA, Abend NS, Hahn CD, Sullivan JE, et al. American clinical neurophysiology society standardized EEG terminology and categorization for the description of continuous EEG monitoring in neonates: report of the American clinical neurophysiology society critical care monitoring committee. *J Clin Neurophysiol*. 2013;30:161–73.
 143. Herman ST, Abend NS, Bleck TP, Chapman KE, Drislane FW, Emerson RG, et al. Consensus statement on continuous EEG in critically ill adults and children, part I: indications. *J Clin Neurophysiol NIH Public Access*. 2015;32:87–95.
 144. Hirsch LJ, Fong MWK, Leitinger M, LaRoche SM, Beniczky S, Abend NS, et al. American clinical neurophysiology society's standardized critical care EEG terminology: 2021 version. *J Clin Neurophysiol NIH Public Access*. 2021;38:1–29.
 145. Libenson MH. Practical approach to electroencephalography. *Spinal Cord*. Elsevier Health Sciences; 2012.
 146. Olejniczak P. Neurophysiologic basis of EEG. *J Clin Neurophysiol LWW*. 2006;23:186–9.
 147. Ng MC, Jing J, Westover MB. A primer on EEG spectrograms. *J Clin Neurophysiol Wolters Kluwer*. 2022;39:177–83.
 148. El-Dib M, Chang T, Tsuchida TN, Clancy RR. Amplitude-integrated electroencephalography in neonates. *Pediatr Neurol*. 2009;41:315–26.
 149. Ng MC, Jing J, Westover MB. Atlas of intensive care quantitative EEG [Internet]. 1st ed. Atlas Intensive Care Quant. EEG. New York: Springer Publishing Company; 2019. <https://connect.springerpub.com/content/book/978-0-8261-9355-1>
 150. Swisher CB, White CR, Mace BE, Dombrowski KE, Husain AM, Kolls BJ, et al. Diagnostic accuracy of electrographic seizure detection by neurophysiologists and non-neurophysiologists in the adult ICU using a panel of quantitative EEG trends. *J Clin Neurophysiol*. 2015;32(4):324–30.
 151. Haider HA, Esteller R, Hahn CD, Westover MB, Halford JJ, Lee JW, et al. Sensitivity of quantitative EEG for seizure identification in the intensive care unit. *Neurology*. 2016;87:935–44.
 152. Foreman B, Claassen J. Quantitative EEG for the detection of brain ischemia. *Crit Care*. 2012;2012:746–58.
 153. Gaspard N. Current clinical evidence supporting the use of continuous EEG monitoring for delayed cerebral ischemia detection. *J Clin Neurophysiol*. 2016;33(3):211–6.

154. Kamitaki BK, Tu B, Wong S, Mendiratta A, Choi H. Quantitative EEG changes correlate with post-clamp ischemia during carotid endarterectomy. *J Clin Neurophysiol.* 2021;38:213–20.
155. Yu Z, Wen D, Zheng J, Guo R, Li H, You C, et al. Predictive accuracy of alpha-delta ratio on quantitative electroencephalography for delayed cerebral ischemia in patients with aneurysmal subarachnoid hemorrhage: meta-analysis. *World Neurosurg.* 2019;126:e510–6.
156. Kamitaki BK, Tu B, Reynolds AS, Schevon CA. Teaching NeuroImages: acute stroke captured on EEG in the ICU: visual and quantitative analysis. *Neurology.* 2019;92(6):e626–7.
157. Alsallom F, Casassa C, Akkineni K, Lin L. Early detection of cerebral herniation by continuous electroencephalography and quantitative analysis. *Clin EEG Neurosci.* 2022;53:133–7.
158. Munjal NK, Bergman I, Scheuer ML, Genovese CR, Simon DW, Patterson CM. Quantitative electroencephalography (EEG) predicting acute neurologic deterioration in the pediatric intensive care unit: a case series. *J Child Neurol.* 2022;37:73–9.
159. Swisher CB, Sinha SR. Utilization of quantitative EEG trends for Critical care continuous EEG monitoring: a survey of neurophysiologists. *J Clin Neurophysiol LWW.* 2016;33:538–44.
160. Mesquita RC, Durduran T, Yu G, Buckley EM, Kim MN, Zhou C, et al. Direct measurement of tissue blood flow and metabolism with diffuse optics. *Philos Trans R Soc A Math Phys Eng Sci.* 2011;369:4390–406. <https://doi.org/10.1098/rsta.2011.0232>.
161. Durduran T, Choe R, Baker WB, Yodh AG. Diffuse optics for tissue monitoring and tomography. *Reports Prog Phys.* 2010;73:076701.
162. Van Meurs KP, Yan ES, Randall KS, Chock VY, Davis AS, Glennon CS, et al. Development of a NeuroNICU with a broader focus on all newborns at risk of brain injury: the first 2 years. *Am J Perinatol.* 2018;35:1197–205.
163. Harvey-Jones K, Lange F, Tachtsidis I, Robertson NJ, Mitra S. Role of optical neuromonitoring in neonatal encephalopathy: current state and recent advances. *Front Pediatr.* 2021;9:1–18.
164. Woodward KE, de Jesus P, Esser MJ. Neuroinflammation and precision medicine in pediatric neurocritical care: multi-modal monitoring of immunometabolic dysfunction. *Int J Mol Sci.* 2020;21:1–21.
165. Gardner Yelton SE, Williams MA, Young M, Fields J, Pearl MS, Casella JF, et al. Perioperative management of pediatric patients with moyamoya arteriopathy. *J Pediatr Intensive Care.* 2021;01(07):2021.
166. Marino BS. New concepts in predicting, evaluating, and managing neurodevelopmental outcomes in children with congenital heart disease. *Curr Opin Pediatr.* 2013;25:574–84.
167. Neshat Vahid S, Panisello JM. The state of affairs of neurologic monitoring by near-infrared spectroscopy in pediatric cardiac critical care. *Curr Opin Pediatr.* 2014;26:299–303.
168. Humblet K, Docquier MA, Rubay J, Momeni M. Multimodal brain monitoring in congenital cardiac surgery: the importance of processed electroencephalogram monitor, NeuroSENSE, in addition to cerebral near-infrared spectroscopy. *J Cardiothorac Vasc Anesth.* 2017;31:254–8.
169. Hyttel-Sorensen S, Greisen G, Als-Nielsen B, Gluud C. Cerebral near-infrared spectroscopy monitoring for prevention of brain injury in very preterm infants. *Cochrane Database Syst Rev.* 2017. <https://doi.org/10.1002/14651858.CD011506.pub2>.
170. Medikonda R, Ong CS, Wadia R, Goswami D, Schwartz J, Wolff L, et al. A review of goal-directed cardiopulmonary bypass management in pediatric cardiac surgery. *World J Pediatr Congenit Hear Surg.* 2018;9:565–72.
171. Zaleski KL, Kussman BD. Near-infrared spectroscopy in pediatric congenital heart disease. *J Cardiothorac Vasc Anesth.* 2020;34:489–500.
172. Houska NM, Schwartz LI. The year in review: anesthesia for congenital heart disease 2019. *Semin Cardiothorac Vasc Anesth.* 2020;24:175–86.
173. Brown KL, Agrawal S, Kirschen MP, Traube C, Topjian A, Pressler R, et al. The brain in pediatric critical care: unique aspects of assessment, monitoring, investigations, and follow-up. *Intensive Care Med.* 2022;48:535–47. <https://doi.org/10.1007/s00134-022-06683-4>.
174. Hunter CL, Oei JL, Suzuki K, Lui K, Schindler T. Patterns of use of near-infrared spectroscopy in neonatal intensive care units: international usage survey. *Acta Paediatr Int J Paediatr.* 2018;107:1198–204.
175. Laws JC, Jordan LC, Pagano LM, Wellons JC, Wolf MS. Multimodal neurologic monitoring in children with acute brain injury. *Pediatr Neurol.* 2022;129:62–71. <https://doi.org/10.1016/j.pediatrneurol.2022.01.006>.
176. Tombolini S, De Angelis F, Correani A, Marchionni P, Monachesi C, Ferretti E, et al. Is low cerebral near infrared spectroscopy oximetry associated with neurodevelopment of preterm infants without brain injury? *J Perinat Med.* 2022;50(5):625–9.
177. Wolf M, Naulaers G, Van BF, Kleiser S, Greisen G. Review: a review of near infrared spectroscopy for term and preterm newborns. *J Near Infrared Spectrosc.* 2012;20:43–55.
178. Dempsey EM, Kooi EMW, Boylan G. It's all about the brain: neuromonitoring during newborn transition. *Semin Pediatr Neurol.* 2018;28:48–59. <https://doi.org/10.1016/j.jspen.2018.05.006>.
179. Jeon GW. Clinical application of near-infrared spectroscopy in neonates. *Neonatal Med.* 2019;26:121–7.
180. Vesoulis ZA, Mintzer JP, Chock VY. Neonatal NIRS monitoring: recommendations for data capture and review of analytics. *J Perinatol.* 2021;41:675–88. <https://doi.org/10.1038/s41372-021-00946-6>.
181. Hansen ML, Hyttel-Sorensen S, Jakobsen JC, Gluud C, Kooi EMW, Mintzer J, et al. Cerebral near-infrared spectroscopy monitoring (NIRS) in children and adults: a systematic review with meta-analysis. *Pediatr Res.* 2022. <https://doi.org/10.1038/s41390-022-01995-z>.
182. Thiele RH, Shaw AD, Bartels K, Brown CH, Grocott H, Heringlake M, et al. American society for enhanced recovery and perioperative quality initiative joint consensus statement on the role of neuromonitoring in perioperative outcomes: cerebral near-infrared spectroscopy. *Anesth Analg.* 2020;131:1444–55.
183. Mitra S, Bale G, Meek J, Tachtsidis I, Robertson NJ. Cerebral near infrared spectroscopy monitoring in term infants with hypoxic ischemic encephalopathy: a systematic review. *Front Neurol.* 2020;11:1–17.
184. Da Dalt L, Parri N, Amigoni A, Nocerino A, Selmin F, Manara R, et al. Italian guidelines on the assessment and management of pediatric head injury in the emergency department. *Ital J Pediatr.* 2018;44:1–41.
185. Jacques SL, Pogue BW. Tutorial on diffuse light transport. *J Biomed Opt.* 2008;13:041302.
186. Matcher SJ, Elwell CE, Cooper CE, Cope M, Delpy DT. Performance comparison of several published tissue near-infrared spectroscopy algorithms. *Anal Biochem.* 1995;227:54–68.
187. Tachtsidis I, Tisdall MM, Pritchard C, Leung TS, Ghosh A, Elwell CE, et al. Analysis of the changes in the oxidation of brain tissue cytochrome-c-oxidase in traumatic brain injury patients during hypercapnoea: a broadband NIRS study. *Adv Exp Med Biol.* 2011;701:9–14.
188. Qin J, Lu R. Measurement of the absorption and scattering properties of turbid liquid foods using hyperspectral imaging. *Appl Spectrosc.* 2007;61:388–96.
189. Bale G, Elwell CE, Tachtsidis I. From Jöbsis to the present day: a review of clinical near-infrared spectroscopy measurements of cerebral cytochrome-c-oxidase. *J Biomed Opt.* 2016;21:091307. <https://doi.org/10.1117/1.JBO.21.9.091307>.
190. Jacques SL. Optical properties of biological tissues: a review. *Phys Med Biol.* 2013;58:R37. <https://doi.org/10.1088/0031-9155/58/11/R37/meta>.
191. Pham TH, Coquoz O, Fishkin JB, Anderson E, Tromberg BJ. Broad bandwidth frequency domain instrument for quantitative tissue optical spectroscopy. *Rev Sci Instrum.* 2000;71:2500–13.
192. Fantini S, Hueber D, Franceschini MA, Gratton E, Rosenfeld W, Stubblefield PG, et al. Non-invasive optical monitoring of the newborn piglet brain using continuous-wave and frequency-domain spectroscopy. *Phys Med Biol.* 1999;44:1543–63.
193. Dean Kurth C, Thayer WS. A multiwavelength frequency-domain near-infrared cerebral oximeter. *Phys Med Biol.* 1999;44:727–40.
194. Chance B, Nioka S, Kent J, McCully K, Fountain M, Greenfield R, et al. Time-resolved spectroscopy of hemoglobin and myoglobin in resting and ischemic muscle. *Anal Biochem.* 1988;174:698–707.
195. Patterson MS, Chance B, Wilson BC. Time resolved reflectance and transmittance for the non-invasive measurement of tissue optical properties. *Appl Opt Soc.* 1989;28:2331–6.
196. Wabnitz H, Jelzow A, Mazurenka M, Steinkellner O, Macdonald R, Milej D, et al. Performance assessment of time-domain optical brain imagers, part 2: nEUROpt protocol. *J Biomed Opt.* 2014;19:086012. <https://doi.org/10.1117/1.JBO.19.8.086012>.
197. Wyatt JS, Cope M, Delpy DT, Richardson CE, Edwards D, Wray S, et al. Quantitation of cerebral blood volume in human infants by near-infrared spectroscopy. *J Appl Physiol.* 1990;68:1086–91.

198. Lange F, Tachtsidis I. Clinical brain monitoring with time domain NIRS: a review and future perspectives. *Appl Sci*. 2019;9(8):1612.
199. Diop M, Kishimoto J, Toronov V, Lee DSC, St. Lawrence K. Development of a combined broadband near-infrared and diffusion correlation system for monitoring cerebral blood flow and oxidative metabolism in preterm infants. *Biomed Opt Exp*. 2015;6:3907–18.
200. Rajaram A, Bale G, Kewin M, Tachtsidis I, Lawrence KS, Diop M. Hybrid broadband NIRS/Diffuse correlation spectroscopy system for simultaneous monitoring of cerebral perfusion and cytochrome c oxidase. In: *Optical tomography and spectroscopy Part F91-T:2588–603*
201. Venkata Sekar SK, Lanka P, Farina A, Mora AD, Andersson-Engels S, Taroni P, et al. Broadband time domain diffuse optical reflectance spectroscopy: a review of systems, methods, and applications. *Appl Sci*. 2019;9(24):5465.
202. Lange F, Dunne L, Hale L, Tachtsidis I. MAESTROS: a multiwavelength time-domain NIRS system to monitor changes in oxygenation and oxidation state of cytochrome-C-oxidase. *IEEE J Sel Top Quantum Electron*. 2019;25:1–12.
203. Boas DA, Yodh AG. Spatially varying dynamical properties of turbid media probed with diffusing temporal light correlation. *J Opt Soc Am A*. 1997;14:192.
204. Durduran T, Yodh AG. Diffuse correlation spectroscopy for non-invasive, micro-vascular cerebral blood flow measurement. *Neuroimage*. 2014;85:5163. <https://doi.org/10.1016/j.neuroimage.2013.06.017>.
205. Boas DA, Dunn AK. Laser speckle contrast imaging in biomedical optics. *J Biomed Opt*. 2010;15:011109.
206. Wu MM, Perdue K, Chan S-T, Stephens KA, Deng B, Franceschini MA, et al. Complete head cerebral sensitivity mapping for diffuse correlation spectroscopy using subject-specific magnetic resonance imaging models. *Biomed Opt Exp*. 2022;13:1131.
207. Buckley EM, Cook NM, Durduran T, Kim MN, Zhou C, Choe R, et al. Cerebral hemodynamics in preterm infants during positional intervention measured with diffuse correlation spectroscopy and transcranial Doppler ultrasound. *Opt Express*. 2009;17:12571.
208. Zhou C, Eucker SA, Durduran T, Yu G, Ralston J, Friess SH, et al. Diffuse optical monitoring of hemodynamic changes in piglet brain with closed head injury. *J Biomed Opt*. 2009;14:034015.
209. Busch DR, Rusin CG, Miller-Hance W, Kibler K, Baker WB, Heinle JS, et al. Continuous cerebral hemodynamic measurement during deep hypothermic circulatory arrest. *Biomed Opt Exp*. 2016;7:3461–70.
210. Jain V, Buckley EM, Licht DJ, Lynch JM, Schwab PJ, Naim MY, et al. Cerebral oxygen metabolism in neonates with congenital heart disease quantified by MRI and optics. *J Cereb Blood Flow Metab*. 2014;34:380–8. <https://doi.org/10.1038/jcbfm.2013.214>.
211. Buckley EM, Hance D, Pawlowski T, Lynch J, Wilson FB, Mesquita RC, et al. Validation of diffuse correlation spectroscopic measurement of cerebral blood flow using phase-encoded velocity mapping magnetic resonance imaging. *J Biomed Opt*. 2012;17:037007. <https://doi.org/10.1117/1.JBO.17.3.037007>.
212. Carp SA, Dai GP, Boas DA, Franceschini MA, Kim YR. Validation of diffuse correlation spectroscopy measurements of rodent cerebral blood flow with simultaneous arterial spin labeling MRI; towards MRI-optical continuous cerebral metabolic monitoring. *Biomed Opt Exp*. 2010;1:553.
213. Ko TS, Mavroudis CD, Baker WB, Morano VC, Mensah-Brown K, Boorady TW, et al. Non-invasive optical neuromonitoring of the temperature-dependence of cerebral oxygen metabolism during deep hypothermic cardiopulmonary bypass in neonatal swine. *J Cereb Blood Flow Metab*. 2020;40:187–203. <https://doi.org/10.1177/0271678X18809828>.
214. Durduran T, Zhou C, Buckley EM, Kim MN, Yu G, Choe R, et al. Optical measurement of cerebral hemodynamics and oxygen metabolism in neonates with congenital heart defects. *J Biomed Opt*. 2010;15:037004. <https://doi.org/10.1117/1.3425884>.
215. Wang D, Parthasarathy AB, Baker WB, Gannon K, Kavuri V, Ko T, et al. Fast blood flow monitoring in deep tissues with real-time software correlators. *Biomed Opt Exp [Internet]*. 2016;7:776.
216. Zhang M, Yang Y, Chen X, Song Y, Zhu L, Gong X, et al. Application of near-infrared spectroscopy to monitor perfusion during extracorporeal membrane oxygenation after pediatric heart surgery. *Front Med*. 2021;8:1–8.
217. Dragojević T, Hollmann JL, Tamborini D, Portaluppi D, Buttafava M, Culver JP, et al. Compact, multi-exposure speckle contrast optical spectroscopy (SCOS) device for measuring deep tissue blood flow. *Biomed Opt Exp*. 2018;9:322.
218. Farzam P, Sutin J, Wu K-C, Zimmermann BB, Tamborini D, Dubb J, et al. Fast diffuse correlation spectroscopy (DCS) for non-invasive measurement of intracranial pressure (ICP) (Conference Presentation). *Clin Transl Neurophoton*. 2017;10050:80–80.
219. Francoeur CL, Lee J, Dangayach N, Gidwani U, Mayer SA. Non-invasive cerebral perfusion monitoring in cardiac arrest patients: a prospective cohort study. *Clin Neurol Neurosurg*. 2020;196:105970. <https://doi.org/10.1016/j.clineuro.2020.105970>.
220. Rajaram A, Milej D, Suwalski M, Kebaya L, Kewin M, Yip L, et al. Assessing cerebral blood flow, oxygenation and cytochrome c oxidase stability in preterm infants during the first 3 days after birth. *Sci Rep*. 2022;12:1–10. <https://doi.org/10.1038/s41598-021-03830-7>.
221. Tabassum S, Ruesch A, Acharya D, Rakkar J, Clark RSB, McDowell MM, et al. Intracranial pressure driven cardiac pulsation waveform changes measured with diffuse correlation spectroscopy. In: *European conference on biomedical optics 2021*. Pp ETu3C-4.
222. Carp SA, Farzam P, Redes N, Hueber DM, Franceschini MA. Combined multi-distance frequency domain and diffuse correlation spectroscopy system with simultaneous data acquisition and real-time analysis. *Biomed Opt Exp*. 2017;8:3993.
223. Tamborini D, Stephens KA, Wu MM, Farzam P, Siegel AM, Shatrovov O, et al. Portable system for time-domain diffuse correlation spectroscopy. *IEEE Trans Biomed Eng*. 2019;66(11):3014–25.
224. Amendola C, Lacerenza M, Buttafava M, Tosi A, Spinelli L, Contini D, et al. A compact multi-distance dcs and time domain nirs hybrid system for hemodynamic and metabolic measurements. *Sensors (Switzerland)*. 2021;21:1–17.
225. Lynch JM, Mavroudis CD, Ko TS, Jacobowitz M, Busch DR, Xiao R, et al. Association of ongoing cerebral oxygen extraction during deep hypothermic circulatory arrest with post-operative brain injury. *Semin Thorac Cardiovasc Surg*. 2021;34(4):1275–84.
226. Busch DR, Baker WB, Mavroudis CD, Ko TS, Lynch JM, McCarthy AL, et al. Noninvasive optical measurement of microvascular cerebral hemodynamics and autoregulation in the neonatal ECMO patient. *Pediatr Res*. 2020;88:925–33. <https://doi.org/10.1038/s41390-020-0841-6>.
227. Giovannella M. BabyLux device: a diffuse optical system integrating diffuse correlation spectroscopy and time-resolved near-infrared spectroscopy for the neuromonitoring of the premature newborn brain. *Neurophotonics*. 2019;6:1.
228. Flanders TM, Lang SS, Ko TS, Andersen KN, Jahnavi J, Flibotte JJ, et al. Optical detection of intracranial pressure and perfusion changes in neonates with hydrocephalus. *J Pediatr*. 2021;236:54-61.e1. <https://doi.org/10.1016/j.jpeds.2021.05.024>.
229. Lin P-Y, Roche-Labarbe N, Dehaes M, Carp S, Fenoglio A, Barbieri B, et al. Non-invasive optical measurement of cerebral metabolism and hemodynamics in infants. *J Vis Exp*. 2013;73:e4379.
230. Irwin D, Dong L, Shang Y, Cheng R, Kudrimoti M, Stevens SD, et al. Influences of tissue absorption and scattering on diffuse correlation spectroscopy blood flow measurements. *Biomed Opt Exp*. 2011;2:1969.
231. Culver JP, Durduran T, Cheung C, Furuya D, Greenberg JH, Yodh AG. Diffuse optical measurement of hemoglobin and cerebral blood flow in rat brain during hypercapnia, hypoxia and cardiac arrest. *Adv Exp Med Biol*. 2003;510:293–7.
232. Culver JP, Durduran T, Furuya D, Cheung C, Greenberg JH, Yodh AG. Diffuse optical tomography of cerebral blood flow, oxygenation, and metabolism in rat during focal ischemia. *J Cereb Blood Flow Metab*. 2003;23:911–24. <https://doi.org/10.1097/01.WCB.0000076703.71.231.BB>.
233. Durduran T, Yu G, Burnett MG, Detre JA, Greenberg JH, Wang J, et al. Diffuse optical measurement of blood flow, blood oxygenation, and metabolism in a human brain during sensorimotor cortex activation. *Opt Lett*. 2004;29:1766.
234. De Carli A, Andresen B, Giovannella M, Durduran T, Contini D, Spinelli L, et al. Cerebral oxygenation and blood flow in term infants during postnatal transition: BabyLux project. *Arch Dis Child Fetal Neonatal Ed*. 2019;104:F648–53.
235. Grant PE, Roche-Labarbe N, Surova A, Themelis G, Selb J, Warren EK, et al. Increased cerebral blood volume and oxygen consumption in neonatal brain injury. *J Cereb Blood Flow Metab*. 2009;29:1704–13. <https://doi.org/10.1038/jcbfm.2009.90>.

236. Nakamura M, Jinnai W, Hamano S, Nakamura S, Koyano K, Chiba Y, et al. Cerebral blood volume measurement using near-infrared time-resolved spectroscopy and histopathological evaluation after hypoxic-ischemic insult in newborn piglets. *Int J Dev Neurosci*. 2015;42:1–9. <https://doi.org/10.1016/j.jdevneu.2015.02.009>.
237. Nakamura S, Koyano K, Jinnai W, Hamano S, Yasuda S, Konishi Y, et al. Simultaneous measurement of cerebral hemoglobin oxygen saturation and blood volume in asphyxiated neonates by near-infrared time-resolved spectroscopy. *Brain Dev*. 2015;37:925–32. <https://doi.org/10.1016/j.braindev.2015.04.002>.
238. Bale G, Mitra S, de Roeve I, Sokolska M, Price D, Bainbridge A, et al. Oxygen dependency of mitochondrial metabolism indicates outcome of newborn brain injury. *J Cereb Blood Flow Metab*. 2019;39:2035–47.
239. Mitra S, Bale G, Highton D, Gunny R, Uria-Avellanal C, Bainbridge A, et al. Pressure passivity of cerebral mitochondrial metabolism is associated with poor outcome following perinatal hypoxic ischemic brain injury. *J Cereb Blood Flow Metab*. 2019;39:118–30.
240. Lynch JM, Ko TS, Busch DR, Newland JJ, Winters ME, Mensah-Brown KG, et al. Pre-operative cerebral hemodynamics from birth to surgery in neonates with critical congenital heart disease. *J Thorac Cardiovasc Surg*. 2018;156:1657–64. <https://doi.org/10.1016/j.jtcvs.2018.04.098>.
241. Vezyroglou A, Hebden P, De Roeve I, Thornton R, Mitra S, Worley A, et al. Broadband-NIRS system identifies epileptic focus in a child with focal cortical dysplasia: a case study. *Metabolites*. 2022;12:260.
242. Mitra S. Predictive role of Cytochrome C Oxidase measured by broadband near infrared spectroscopy as a real time bio marker of newborn brain injury. Thesis. 2018.
243. Ferradal SL, Yuki K, Vyas R, Ha CG, Yi F, Stopp C, et al. Non-invasive assessment of cerebral blood flow and oxygen metabolism in neonates during hypothermic cardiopulmonary bypass: feasibility and clinical implications. *Sci Rep*. 2017;7:1–9. <https://doi.org/10.1038/srep44117>.
244. Mavroudis CD, Ko T, Volk LE, Smood B, Morgan RW, Lynch JM, et al. Does supply meet demand? A comparison of perfusion strategies on cerebral metabolism in a neonatal swine model. *J Thorac Cardiovasc Surg* [Internet]. 2022;163:e47-58. <https://doi.org/10.1016/j.jtcvs.2020.12.005>.
245. Ko TS, Slovis J, Volk L, Mavroudis CD, Morgan RW, Breimann J, et al. Non-invasive measurement of cerebral tissue oxygen extraction fraction is correlated with microdialysis brain injury biomarkers during extracorporeal cardiopulmonary resuscitation. *Circulation*. 2020. https://doi.org/10.1161/circ.142.suppl_4.153.
246. Ko TS, Mavroudis CD, Morgan RW, Baker WB, Marquez AM, Boorady TW, et al. Non-invasive diffuse optical neuromonitoring during cardiopulmonary resuscitation predicts return of spontaneous circulation. *Sci Rep*. 2021;11:3828.
247. White B, Ko T, Morgan RW, Jahnvi J, Benson E., Roberts AL, et al. Low frequency power in cerebral blood flow through cardiac arrest and recovery in a swine model. In: Yang VXD, Kainerstorfer JM, editors. *Optical techniques in neurosurgery, neurophotonics, and optogenetics. SPIE*; 2021. p 3. <https://doi.org/10.1117/12.2578832.full>. Accessed 29 May 2022.
248. Holper L, Mitra S, Bale G, Robertson N, Tachtsidis I. Prediction of brain tissue temperature using near-infrared spectroscopy. *Neurophotonics*. 2017;4:021106. <https://doi.org/10.1117/1.NPh.4.2.021106>.
249. Sekhon MS, Ainslie PN, Griesdale DE. Clinical pathophysiology of hypoxic ischemic brain injury after cardiac arrest: a “two-hit” model. *Crit Care*. 2017;21:1–10.
250. Hayman EG, Patel AP, Kimberly WT, Sheth KN, Simard JM. Cerebral edema after cardiopulmonary resuscitation: a therapeutic target following cardiac arrest? *Neurocrit Care*. 2018;28:276–87.
251. Baker WB, Parthasarathy AB, Gannon KP, Kavuri VC, Busch DR, Abramson K, et al. Noninvasive optical monitoring of critical closing pressure and arteriole compliance in human subjects. *J Cereb Blood Flow Metab*. 2017;37:2691–705.
252. Ruesch A, Yang J, Schmitt S, Acharya D, Smith MA, Kainerstorfer JM. Estimating intracranial pressure using pulsatile cerebral blood flow measured with diffuse correlation spectroscopy. *Biomed Opt Exp*. 2022;13:710.
253. Fischer JB, Ghouse A, Tagliabue S, Maruccia F, Rey-Perez A, Báguena M, et al. Non-invasive estimation of intracranial pressure by diffuse optics: a proof-of-concept study. *J Neurotrauma*. 2020;37:2569–79.
254. Wu K, Sunwoo J, Sheriff F, Farzam PYPY, Farzam PYPY, Orihuela-Espina F, et al. Validation of diffuse correlation spectroscopy measures of critical closing pressure against transcranial Doppler ultrasound in stroke patients. *J Biomed Opt*. 2021;26:036008.
255. Cardim D, Robba C, Bohdanowicz M, Donnelly J, Cabella B, Liu X, et al. Non-invasive monitoring of intracranial pressure using transcranial doppler ultrasonography: is it possible? *Neurocrit Care*. 2016;25:473–91.
256. Ruesch A, Schmitt S, Yang J, Smith MA, Kainerstorfer JM. Fluctuations in intracranial pressure can be estimated non-invasively using near-infrared spectroscopy in non-human primates. *J Cereb Blood Flow Metab*. 2020;40:2304–14.
257. Rhee CJ, da Costa CS, Austin T, Brady KM, Czosnyka M, Lee JK. Neonatal cerebrovascular autoregulation. *Pediatr Res*. 2018;84:602–10. <https://doi.org/10.1038/s41390-018-0141-6>.
258. Donnelly JE, Young AMH, Brady K. Autoregulation in paediatric TBI: current evidence and implications for treatment. *Child's Nerv Syst Child's Nervous Syst*. 2017;33:1735–44.
259. Benninger KL, Inder TE, Goodman AM, Cotten CM, Nordli DR, Shah TA, et al. Perspectives from the society for pediatric research. neonatal encephalopathy clinical trials: developing the future. *Pediatr Res*. 2021;89:74–84. <https://doi.org/10.1038/s41390-020-0859-9>.
260. Fantini S, Sassaroli A, Tgavalekos KT, Kornbluth J. Cerebral blood flow and autoregulation: current measurement techniques and prospects for noninvasive optical methods. *Neurophotonics*. 2016;3:031411.
261. Vu EL, Brady K, Hogue CW. High-resolution perioperative cerebral blood flow autoregulation measurement: a practical and feasible approach for widespread clinical monitoring. *Br J Anaesth*. 2022;128:405–8. <https://doi.org/10.1016/j.bja.2021.12.013>.
262. Kooi EMW, Verhagen EA, Elting JWJ, Czosnyka M, Austin T, Wong FY, et al. Measuring cerebrovascular autoregulation in preterm infants using near-infrared spectroscopy: an overview of the literature. *Expert Rev Neurother* [Internet]. 2017;17:801–18. <https://doi.org/10.1080/14737175.2017.1346472>.
263. Buckley EM, Goff DA, Durduran T, Kim MN, Mesquita RC, Hedstrom G, et al. Post-surgical cerebral autoregulation in neonates with congenital heart defects monitored with diffuse correlation spectroscopy. *Biomed Opt 3-D Imaging* [Internet]. Optica Publishing Group; 2010. p. BSuD71. <http://opg.optica.org/abstract.cfm?URI=BIOMED-2010-BSuD71>
264. Baker WB, Balu R, He L, Kavuri VC, Busch DR, Amendolia O, et al. Continuous non-invasive optical monitoring of cerebral blood flow and oxidative metabolism after acute brain injury. *J Cereb Blood Flow Metab*. 2019;39(8):1469–85.
265. Forti RM, Favilla CG, Cochran JM, Baker WB, Detre JA, Kasner SE, et al. Transcranial optical monitoring of cerebral hemodynamics in acute stroke patients during mechanical thrombectomy. *J Stroke Cerebrovasc Dis*. 2019;28:1483–94.
266. Parthasarathy AB, Gannon KP, Baker WB, Favilla CG, Balu R, Kasner SE, et al. Dynamic autoregulation of cerebral blood flow measured non-invasively with fast diffuse correlation spectroscopy. *J Cereb Blood Flow Metab*. 2018;38:230–40.
267. Selb J, Wu K-C, Sutin J, Lin P-Y, Farzam P, Becek S, et al. Prolonged monitoring of cerebral blood flow and autoregulation with diffuse correlation spectroscopy in neurocritical care patients. *Neurophotonics*. 2018;5:1. <https://doi.org/10.1117/1.NPh.5.4.045005.full>.
268. Gregori-Pla C, Mesquita RC, Favilla CG, Busch DR, Blanco I, Zirak P, et al. Blood flow response to orthostatic challenge identifies signatures of the failure of static cerebral autoregulation in patients with cerebrovascular disease. *BMC Neurol*. 2021;21:1–12.
269. Bale G, Mitra S, De Ri, Chan M, Caicedo-dorado A, Meek J, et al. Inter-relationship between broadband NIRS measurements of cerebral cytochrome C oxidase and systemic changes indicates injury severity in neonatal encephalopathy. *Oxyg Transp to Tissue XXXVIII*. 2016. <https://doi.org/10.1007/978-3-319-55231-6>.
270. Hwang M. Introduction to contrast-enhanced ultrasound of the brain in neonates and infants: current understanding and future potential. *Pediatr Radiol*. 2019;49(2):254–62.
271. Forti RM, Ko TS, Laurent GH, Hobson J, Benson E, Morton S, et al. Optical assessment of edema, perfusion, and oxygen metabolism after severe confusional traumatic brain injury: preliminary results in a swine-model. *Opt Biophotonics Congr Biomed Opt* 2022. Fort Lauderdale, FL; 2022. p. BS3C.5.